NASA Technical Memorandum

82787

Exhaust Emissions Survey of a Turbofan Engine for Flame-Holder- and Swirl-Type Augmentors at Simulated Altitude Flight Conditions

John E. Moss, Jr.
Lewis Research Center
Cleveland, Ohio

October 1981

NASA

SUMMARY

Carbon monoxide (CO), total oxides of nitrogen (NO_x), unburned hydrocarbons (HC), and carbon dioxide (CO_2) emissions from an F100(2) afterburning two-spool turbofan engine at simulated flight conditions are reported herein. Tests were run for two augmentor configurations - Bill of Material, a flame holder design, and partial swirl, flame holder for fan duct air and swirled flow for core air. Emission tests were run at Mach 0.8 at altitudes of 10.97 and 13.71 km (36 000 and 45 000 ft), and at Mach 1.2 at 13.71 km (45 000 ft). For each flight condition, emission measurements were made for one, two, or three power levels from intermediate power (nonafterburning) through maximum afterburning. Emission measurements were made using a single point gas sample probe traversed across the horizontal diameter of the exhaust nozzle.

The data showed that emissions vary with flight speed, altitude, power level, and radial position across the nozzle. Carbon monoxide emissions were low for intermediate power and partial afterburning, but increased sharply at maximum afterburning power. At maximum afterburning, there were regions of NO_x deficiency in regions of high CO for both augmentor configurations. Unburned hydrocarbon emissions were low for most of the simulated flight conditions. Emissions of CO_2 were proportional to local fuel-air ratio for all conditions.

INTRODUCTION

Testing of an F100(2) afterburning two-spool turbofan engine was conducted in an altitude facility to determine the oxides of nitrogen, unburned hydrocarbon, carbon monoxide, and carbon dioxide emissions at simulated flight conditions. Tests were run for two augmentor configurations, Bill of Material and partial swirl. For both configurations, emission tests were run at Mach 0.8 at altitudes of 10.97 and 13.71 km (36 000 and 45 000 ft), and at Mach 1.2 at 13.71 km (45 000 ft). For each simulated flight condition, emission measurements were made for one, two, or three power levels from intermediate power (nonafterburning) through maximum afterburning.

Emission measurements from aircraft turbine engines, and in particular afterburning engines, at high-altitude supersonic flight conditions are needed to answer questions about the environmental impact of high performance aircraft. Other exhaust emissions surveys previously reported on afterburning turbojet and turbofan engines can be found in references 1 to 7.

This investigation was conducted in the Propulsion Systems Laboratory at the NASA Lewis Research Center. The purpose of this study was to measure and compare the exhaust emissions from a Bill of Material (flame-holder-type) augmentor and a partial swirl (flame holder for fan duct air and swirl flow for core air) augmentor. The results of an exhaust emission survey of an F100(1), Bill of Material augmentor, were reported in reference 1. As stated, this survey was made with an F100(2) engine. The F100(2) engine had increased cooling flow to the turbine, tailored spray rings, and an extended exit splitter. The simulated flight conditions in these surveys were not identical; therefore, the results are not directly comparable.

APPARATUS

The F100(2) two-spool turbofan engine used in this investigation is shown installed in the test cell where this evaluation was performed (fig. 1). The F100 is a 111-kn (25 000-lbf) thrust class, high overall pressure ratio (23:1), low bypass ratio (0.71:1) engine. This engine has a mixed-flow afterburner with V-gutter, flame holders, and fuel spray rings. For the partial swirl augmentor, the core swirl was achieved by cutting back the turbine exit vanes (recambered fixed exit guide vanes) and removing the flame holder in the core stream (fig. 2(a)). Photographs of the Bill of Material and partial swirl augmentors are shown in figures 2(b) and (c), while the engine instrumentation locations used in this evaluation are shown in figure 2(d). A more complete description of the engine can be found in reference 8.

INSTALLATION

The engine installation in the altitude test chamber was a conventional direct-connect type shown in figure 1. Conditioned air required to simulate the selected flight conditions was provided by the facility and the engine exhaust pressure level required to simulate flight conditions was maintained. Engine exhaust gases were captured by a water-cooled collector to prevent recirculation in the test chamber. These tests were run using JP-4 fuel (MIL-T-56246).

GAS SAMPLING SYSTEM

A single-point, traversing, water-cooled gas-sample probe was used in this study. The traversing mechanism was capable of translating the probe ±60 cm horizontally and ±20 cm vertically from the engine centerline. A photograph and a schematic of the sensor area of the probe are shown in figures 3(a) and (b). The gas-sampling probe has an inside diameter of 0.72 cm (0.28 in.) and extended 1.9 cm (0.75 in.) forward of the probe support. The gas sample line was water-cooled for a distance of 8 cm (3.2 in.) from the probe tip. From this point the sample line inside diameter was 0.82 cm (0.32 in.) and water-cooled an additional length of 30 cm (12 in.).

A total pressure probe was mounted 2.5 cm (1.0 in.) above the sample probe, and three unshielded iridium/iridium-rhodium thermocouples were mounted 2.5 cm (1.0 in.) and 5.0 cm (2.0 in.) below and 5 cm (2 in.) above the gas sample probe.

A schematic of the gas analysis system is shown in figure 4(a). Approximately 10 m of 0.95-cm stainless-steel line was used to transport the sample to the analyzers. To prevent condensation of water and to minimize adsorption-desorption effects of hydrocarbon compounds, the line was heated with steam at 428 K. Four heated metal bellows pumps were used to supply sufficient gas sample pressure (17 N/cm^2) to operate the analytical instruments. The gas sample line residence time was less than 2 sec for all test conditions.

GAS ANALYSIS INSTRUMENTATION

Four commercially available instruments, along with associated peripheral equipment necessary for sample conditioning and instrument calibration comprised the exhaust-gas analysis system (fig. 4(b)).

The hydrocarbon (HC) content of the exhaust gas was measured on a wet basis, using a Beckman Instruments Model 402 Hydrocarbon Analyzer. This instrument is of the flame ionization detector type. Both carbon monoxide (CO) and carbon dioxide (CO_2) were measured dry, using analyzers of the nondispersive infrared (NDIR) type. These instruments were Beckman Instruments Model 315B. The concentration of the oxides of nitrogen (NO_x) was measured on a dry basis using a Thermo Electron Corporation Model 10A Chemiluminescence Analyzer. This instrument includes a stainless steel thermal converter to reduce nitrogen dioxide (NO_2) to nitric oxide (NO). Exhaust gas constituents which were measured on a dry basis (CO, CO_2, and NO_x) were corrected for inlet air humidity and water vapor from combustion, and are reported herein on a wet basis.

The exhaust emission data measured by the analytical instruments were recorded and processed by an on-line facility computer. This computer was also used to control the traverse of the gas sample probe and to determine the nozzle exit diameter.

TEST CONDITIONS AND PROCEDURES

Exhaust emission surveys were conducted at simulated altitude conditions of 10.97 and 13.71 km (36 000 and 45 000 ft) at Mach 0.8 for the Bill of Material and the partial swirl augmentor configurations. Surveys were also made at 13.71 km (45 000 ft) at Mach 1.2 for both configurations. These test conditions were representative of typical subsonic and supersonic aircraft operating points. This choice of conditions gives a variation in altitude at a constant subsonic Mach number and a variation in simulated Mach number at a constant altitude for two augmentor configurations. The test points and nominal inlet conditions are presented in table I. Conditioned air was supplied to the plenum at the desired pressure and temperature. The test chamber was maintained at the pressure required for true simulation of the selected altitude condition. This pressure resulted in the nozzle being choked for all survey data presented.

Emissions surveys were made at one, two or three power settings at each simulated flight condition. Power levels included intermediate (maximum power, nonafterburning), partial afterburning (afterburning zones 1, 2 and 3) and maximum afterburning (all five zones of afterburning); see figure 4(d). Gas sampling surveys were made slightly downstream of the nozzle exit plane. For the nominal maximum afterburning condition, the nozzle was near wide open and the axial distance from the nozzle lip downstream to the survey plane was 5.6 cm (2.2 in.). At the partial afterburning power level, the nozzle area decreased from maximum and the axial distance from the nozzle lip to the survey plane was 6.4 cm (2.5 in.). At intermediate power the nozzle was near its minimum area and the distance from nozzle lip to survey plane was 8.8 cm (3.5 in.).

The exhaust nozzle diameter was obtained using the survey rake in conjunction with two nozzle-mounted air jets. Aft-facing high pressure air

jets were mounted on two diametrically opposite divergent nozzle leaves coinciding with the horizontal survey diameter. Just prior to a gas sample survey a continuous traverse was made and the position of the air jets marking the nozzle exit diameter were noted as pressure spikes sensed by the total pressure probe of the survey rake. The nozzle exit radius (R_8) for each condition was obtained from these measurements except that at Mach 0.8 and 13.71 km, Bill of Material augmentor, the measured exhaust nozzle diameter was not correct, as the emission probe was not in the exhaust stream for part of the survey. For this case, R_8 was adjusted based on examination of the data (also see next section).

Surveys were made across the horizontal diameter of the exhaust nozzle. Twenty-one data points were recorded for afterburning to delineate the steep gradients in the emission profile. This resulted in a nominal spacing of 4.8 cm (1.9 in.) for maximum afterburning and 4.3 cm (1.7 in.) for partial afterburning. A twenty-one data point traverse required approximately 30 min to complete. Eleven data points were recorded for nonafterburning as the gradients in the emission profiles were less steep. The nominal data point spacing at intermediate power was 6.6 cm (2.6 in.).

RESULTS AND DISCUSSION

Profile Data

Exhaust profile data are shown in figures 5 to 11. A complete tabulation of the experimental data obtained in this investigation is included in appendix A. This appendix also contains the average data (mass weighted and area integrated). A list of symbols used in this report is presented in appendix B. CO, CO_2, and NO_x concentrations are given as parts per million by volume (ppmv), and the HC concentrations are given as parts per million carbon by volume (ppmC). The horizontal axes in the figures are the radial distances from the centerline nondimensionalized by the measured nozzle exit radius (R_8) for each test. This radius varies with flight condition and engine power level. Note that at Mach 0.8 and 13.71 km, for afterburning tests with the Bill of Material augmentor, the measured R_8 radii were incorrect and have been adjusted. These data are plotted as dashed (---) lines in the figures. Data are tabulated in appendix A "as measured".

Exhaust total temperature. - The total temperature distribution across the nozzle at each power level is shown in figure 5. At intermediate power, the temperature distribution is nearly uniform across the exhaust plane. For partial afterburning, the temperature profiles show twin regions of high temperature. The low temperature in the center region is only slightly greater than the center value without afterburning, and indicates that there was very little combustion in the wake behind the centerbody. For maximum afterburning, the temperature profile is nearly flat at high temperature levels, indicating radially uniform combustion. The temperature profiles were not affected significantly by Mach number, altitude, or augmentor configuration.

Fuel-air ratio. - The local fuel-air ratio (FAREMISS) calculated from the gas sample measurements using the relationship in reference 9 are shown in figure 6. The similarity of the fuel-air ratio and the temperature pro-

files and the increase in the average temperature with increasing power level was expected, since increasing the fuel-air ratio should increase the temperature for all fuel-air ratios less than stoichiometric. The local fuel-air ratio profiles were not affected significantly by Mach number, altitude, or augmentor configuration.

Carbon monoxide. - The variations of carbon monoxide (CO) emissions with flight conditions for each power level are shown in figure 7. Except for two data points, CO emissions for intermediate and partial afterburning power were less than 2000 ppmv for all simulated flight conditions.

For maximum afterburning, CO emission profiles are highly nonuniform for all flight conditions as shown in figures 7(c) to (e). Except for the swirl augmentor at Mach 0.8 and 13.71 km, all maximum afterburning CO emissions exhibited twin peaks of approximately 12 000 ppmv in the fan stream. A maximum CO concentration of 14 400 ppmv was measured in the fan stream of the partial swirl augmentor at Mach 0.8 and 13.71 km. It is apparent in figures 9(c) to (e) that there are significant differences between the core stream levels for the two augmentor types with concentration for the swirl augmentor consistently less than for the Bill of Material augmentor, but still substantially higher than at intermediate power or partial afterburning power. Note that the local fuel-air ratios were approaching stoichiometric in the high CO concentration regions, and the high CO levels may represent an approach to equilibrium CO, rather than combustion inefficiency.

Although the data shown in figure 7 are typical, significant differences in distribution do occur for different engines, flight speeds, altitudes, etc., (e.g., the results reported in ref. 1 which also had a Bill of Material augmentor had very low CO emissions in the center of the exhaust nozzle).

Hydrocarbon. - Measured hydrocarbon emissions were near zero for all radii for nonafterburning conditions (fig. 8(a)). For the partial swirl augmentor at partial afterburning, the hydrocarbon emissions were near zero for all radii (R/R_8) greater than 0.6 or less than 0.8, whereas for the Bill of Material augmentor, hydrocarbon concentrations up to 3000 ppmC were measured in this region. As seen in figure 8(b), hydrocarbon emissions levels were typically higher at outboard radii than in the center for both augmentors. At maximum afterburning, the hydrocarbon emissions were less than 1000 ppmC for all simulated flight conditions for both augmentors (fig. 8(c)).

Oxides of nitrogen. - The variations of the oxides of nitrogen (NO_x) emissions with flight condition at each power level are shown in figure 9. For intermediate power at Mach 0.8 and 13.71 km (fig. 9(a)), the peak oxides of nitrogen emissions were about the same for both augmentors. For the same power level and simulated flight speed, results from the engine with the Bill of Material Augmentor showed that as altitude decreased, NO_x emissions increased.

At Mach 1.2 and 13.71 km and intermediate power (nonafterburning), the NO_x emissions were greater for the test with the Bill of Material augmentor than for the test with the partial swirl augmentor (fig. 9(b)). Note that this is in contrast to the near equality of NO_x levels between the Bill of Material and swirl augmentor test at Mach 0.8 and 13.71 km (fig.

9(a)). At intermediate power the NO_x emissions increased with Mach number at 13.71 km for both augmentors (figs. 9(a) and (b)).

For partial afterburning power, the same trends are observed as at intermediate power NO_x emissions for Mach 0.8 at 13.71 km were approximately the same for both augmentor configurations (fig. 9(c)), but for Mach 1.2 at 13.71 km, the NO_x emissions were greater for the Bill of Material augmentor than for the partial swirl augmentor (fig. 9(d)). NO_x emissions increased with increased Mach number at 13.71 km at partial afterburning power for both augmentors. The measured oxides of nitrogen concentrations at maximum afterburning are shown in figures 9(e) to (g). At maximum afterburning, there are regions of NO_x deficiency in regions of very high CO. For example, at maximum afterburning, Mach 1.2 at 13.71 km, Bill of Material augmentor, the CO emissions have twin peaks of high CO concentrations, and high CO emissions at the center of the exhaust nozzle (fig. 7(e)). The NO_x emissions for this simulated flight condition are near zero for most radii (fig. 9(g)). The only maximum afterburning condition for which measured NO_x was consistantly high was with the partial swirl augmentor at Mach 0.8 and 13.71 km. Note in figure 7(d) that CO levels were less than 3000 ppmv at all radii for this condition. The correlation between high CO and low measured NO_x is obvious at the other conditions also, and, in fact, can be seen in the results of previous investigations, for example, references 1 and 7. Although in the latter, simultaneous NO and NO_x measurements were made, and NO was used whenever measured NO_x was less than NO.

These results suggest that the low NO_x levels observed in the tests reported here are a result of interaction with high CO in the thermal converter. Simultaneous NO measurements were not made in this study, thus precluding any further examination or conclusions regarding the source of the NO_x deficiency using the present results. With the possible exception of the NO_x concentrations at Mach 0.8 and 13.71 km, we do not believe that the NO_x levels reported here for maximum afterburning are representative of actual concentrations in the exhaust.

Carbon dioxide. - The variations of carbon dioxide with flight conditions at each power level are shown in figure 10. The CO_2 emission profiles are similar, as expected, to the fuel-air ratio profiles (fig. 6) and showed little variations with Mach number, altitude, or augmentor configuration. The CO_2 emission profiles are radially uniform at intermediate power; however, at partial afterburning, the CO_2 profiles have twin regions of high emissions. The CO_2 emission profiles for maximum afterburning are also radially uniform.

Exhaust total pressure. - The total exhaust pressure profiles are shown in figure 11. At intermediate power, the measured exhaust total pressure, Pt_8, was greater for the partial swirl augmentor; however, for partial and maximum afterburning power, the Bill of Material augmentor had a higher exhaust total pressure.

Correlation with Local Fuel-Air Ratio

As discussed previously, the measured values of CO, NO_x, HC, and CO_2, at each radial location were used to calculate emission based fuel-air ratios (FAREMISS; see fig. 6). The mass and area weighted average

FAREMISS values are consistently lower than the metered fuel-air ratios (FAABT) as seen in figure 12.

Figures 13 to 16 show the emissions data plotted against the local fuel-air ratio for all flight conditions and power levels tested. Carbon monoxide (fig. 13) was low for local fuel-air ratios (FAREMISS) less than 0.05, but increased sharply for most local fuel-air ratios greater than this value.

Carbon dioxide emissions increased linearly with increased values of local fuel-air ratios (fig. 14) except for deviations at high overall afterburner fuel-air ratios (F/A) in regions of high carbon monoxide.

Hydrocarbons were essentially zero for all intermediate power (nonafterburning) conditions and showed considerable scatter in afterburning (fig. 15). No correlation between the hydrocarbon emission and local fuel-air ratio (FAREMISS) is apparent.

The oxides of nitrogen (NO_x) emissions increased linearly with FAREMISS at intermediate power conditions (fig. 16). However, this increase in fuel-air ratio was not observed in afterburning, suggesting that very little, if any, additional NO_x is produced in the augmentor. The low NO_x concentrations at the higher fuel-air ratios are data for the NO_x deficient regions in the profiles at maximum afterburning.

The combustion efficiencies calculated from gas sample data with and without afterburning are shown in table II. The local concentration data (CO, CO_2, HC, and NO_x) were mass weighted and area integrated to obtain average concentrations. These average concentrations were used to calculate combustion efficiencies. For the test conditions reported the efficiencies did not vary with changes in simulated flight conditions.

CONCLUDING REMARKS

Gaseous emissions were measured at simulated flight conditions for an F100(2) afterburning two-spool turbofan engine. For each flight condition, detailed concentration profile measurements were made for one, two or three engine power levels from intermediate (nonafterburning) through maximum afterburning. These measurements were made on the horizontal diameter at the engine exhaust nozzle exit using a single-point traversing sample probe. The data showed that emissions vary with flight speed, altitude, power level, and radial position across the nozzle. The principal results of this investigation are as follows:

1. Total temperature, fuel-air ratio, and CO_2 emissions showed little variations with Mach number, altitudes, or augmentor configuration.
2. The hydrocarbon emissions were near zero for most of the simulated flight conditions.
3. Carbon monoxide emissions were low for intermediate and partial afterburning power but increased sharply at maximum afterburning.
4. There were significant differences between the core stream CO emission levels for the two augmentors, with the core stream CO concentrations consistently higher for the Bill of Material augmentor
5. At Mach 0.8 and 13.71 km, oxides of nitrogen emissions were nearly the same for both augmentors at both intermediate and partial afterburning power, but at Mach 1.2 and 13.71 km, NO_x emissions were less with the partial swirl augmentor than for the Bill of Material augmentor for both intermediate and partial afterburning power.

6. The NO_x emissions increased with Mach number for both augmentors for intermediate and partial afterburning power at 13.71 km.

7. At maximum afterburning, there were regions of NO_x deficiency in regions of very high CO for both augmentor configurations.

8. While there were differences between the Bill of Material (flame holder type) augmentor and the partial swirl augmentor with respect to emissions, these differences were not considered significant.

APPENDIX A - COMPLETE TABULATION OF EXPERIMENTAL DATA

The engine inlet conditions and the exhaust profile data for all flight conditions and power levels are given in tables A-I to A-VI in this appendix.

TABLE A-I. - ENGINE INLET TEST CONDITIONS AND EXHAUST PROFILE DATA FOR CONDITION 1

[Mach 0.8 at 10.97 km (36 000 ft); maximum afterburning power; engine inlet temperature, T_2 = 244 K; engine inlet pressure Pt_2 = 3.49 N/cm^2; metered fuel-air ratio FAABT = 0.063; exhaust nozzle radius R_8 = 46.11 cm; partial swirl augmentor.]

R/R_8	COPPM	CO_2PPM	HCPPM	NO_xPPM	FAREMISS	TT_8, K	Pt_8, N/cm^2
-1.00	333	16 403	4	14	0.0082	561	3.05
-0.895	1 004	46 759	72	40	.0238	1401	8.32
-.794	2 397	103 960	9	120	.0548	1940	8.90
.695	11 864	90 007	257	4	.0528	1932	8.83
-.598	6 476	101 450	13	1	.0558	1914	8.53
.501	1 870	106 200	0	1	.0557	1921	8.24
-.401	1 542	106 540	0	221	.0557	1943	8.15
.306	2 379	106 880	0	231	.0564	1956	8.03
-.213	3 036	106 400	0	206	.0565	1961	7.86
.115	1 526	106 560	0	204	.0557	1960	7.89
0.0	582	96 016	0	202	.0495	1928	7.12
.106	697	102 630	0	209	.0531	1968	7.98
.201	2 124	106 760	0	224	.0562	1972	8.07
.302	1 625	107 020	0	228	.0560	1959	8.05
.398	1 554	106 860	0	229	.0559	1953	8.21
.496	3 438	105 790	0	221	.0564	1947	8.53
.590	8 607	97 896	11	26	.0551	1936	8.82
.687	12 107	89 105	148	1	.0524	1927	8.92
.785	12 532	87 629	199	1	.0518	1948	8.83
.907	650	87 351	0	78	.0449	1742	8.21
1.00	785	38 378	3	33	.0194	845	6.53
Average	4 560	86 198	58	80	0.0396	----	-----

TABLE A-II. - ENGINE INLET CONDITIONS AND EXHAUST PROFILE DATA FOR CONDITION 2

[Mach 0.8 at 10.97 km (36 000 ft).]

(a) Intermediate (nonafterburning) power; engine inlet temperature T_2 = 245 K; engine inlet pressure Pt_2 = 3.37 = N/cm^2; metered fuel-air ratio FAABT = 0.012; exhaust nozzle radius R_8 = 28.89 cm; Bill of Material augmentor.

R/R_8	COPPM	CO_2PPM	HCPPM	NO_xPPM	FAREMISS	TT_8, K	Pt_8, N/cm^2
-1.00	51	9 934	3	40	0.0048	493	8.65
0.801	327	17 991	3	67	.0090	613	9.73
-.603	824	33 223	2	140	.0168	785	10.43
.400	923	38 127	2	165	.0194	847	10.60
-.195	21	37 283	2	165	.0185	849	10.57
.005	14	37 152	2	165	.0184	844	8.43
.201	15	37 861	2	165	.0188	852	10.55
.409	15	37 394	2	167	.0185	840	10.52
.599	21	33 480	2	152	.0166	789	10.44
.810	5	27 537	2	128	.0136	669	9.97
1.00	9	17 220	3	74	.0084	553	18.15
Average	244	26 480	2	115	0.0120	----	-----

TABLE A-II. - Concluded.

(b) Maximum afterburning power; engine inlet temperature T_2 = 245; engine inlet pressure Pt_2 = 3.43 N/cm^2; metered fuel-air ratio FAABT = 0.061; exhaust nozzle radius R_8 = 44.25 cm; Bill of Material augmentor.

R/R_8	COPPM	CO_2PPM	HCPPM	NO_xPPM	FAREMISS	TT_8, K	Pt_8, N/cm^2
-1.038	999	35 183	508	32	0.0182	539	6.27
-0.928	347	83 526	12	81	.0427	965	8.70
-.838	8 686	95 492	41	53	.0538	1053	9.27
.738	11 407	89 441	124	12	.0521	1038	9.42
-.632	9 677	93 950	37	12	.0536	1034	9.29
-.537	5 432	101 590	11	12	.0553	1025	9.04
-.424	1 452	104 600	9	12	.0546	1025	8.89
-.332	4 944	102 390	9	34	.0554	1030	8.79
-.223	8 962	95 143	11	12	.0538	1034	8.80
-.129	6 984	99 201	9	12	.0549	1048	9.42
-.035	4 950	102 320	8	11	.0554	1058	8.95
.062	6 395	100 220	9	11	.0551	1048	9.41
.175	7 447	98 186	10	11	.0546	1037	8.83
.265	3 054	103 650	8	11	.0550	1030	8.85
.368	568	97 493	8	200	.0503	1000	8.96
.472	670	98 311	8	212	.0508	995	9.03
.569	2 366	103 460	9	224	.0545	1021	9.14
.671	7 772	97 687	11	35	.0545	1041	6.84
.771	8 466	96 321	12	12	.0541	1043	7.59
.867	889	88 670	8	110	.0457	947	7.37
1.038	423	22 764	12	31	.0114	369	1.91
Average	4 551	89 700	31	64	.0411	----	-----

TABLE A-III. - ENGINE INLET CONDITIONS AND EXHAUST

PROFILE DATA FOR CONDITION 3

[Mach 0.8 at 13.71 km (45 000 ft).]

(a) Intermediate (nonafterburning) power; engine inlet temperature T_{2} = 242 K; engine inlet pressure Pt_{2} = 2.22 N/cm^2; metered fuel-air ratio FAABT = 0.013; exhaust nozzle radius R_{8} = 30.65 cm; partial swirl augmentor.

R/R_8	COPPM	CO_2PPM	HCPPM	NO_xPPM	FAREMISS	TT_8, K	Pt_8, N/cm^2
-0.998	118	21 728	23	73	0.0107	648	12.01
-.816	111	27 616	16	85	.0137	742	13.08
-.622	100	31 968	13	108	.0158	804	13.80
-.413	115	34 973	12	131	.0174	833	16.96
-.206	118	36 947	13	144	.0184	851	13.04
0.0	118	37 148	10	145	.0185	855	13.53

TABLE A-III. - Continued.

(b) Partial afterburning power; engine inlet temperature T_2 = 240 K; engine inlet pressure Pt_2 = 2.19 N/cm^2; metered fuel-air ratio FAABT = 0.033; exhaust nozzle radius R_8 = 38.35 cm; partial swirl augmentor.

R/R_8	COPPM	CO_2PPM	HCPPM	NO_xPPM	FAREMISS	TT_8, K	Pt_8, N/cm^2
-0.997	772	20 314	84	18	0.0104	659	14.59
.907	1 316	30 397	3112	8	.0173	1069	8.69
-.805	1 640	51 818	1110	59	.0273	1348	7.93
.711	1 169	62 714	344	75	.0323	1498	7.46
-.594	748	66 172	66	117	.0388	1474	7.79
.506	608	62 157	35	166	.0316	1371	6.90
-.406	494	57 353	32	164	.0290	1287	7.06
.294	401	53 112	36	164	.0268	1178	6.54
-.199	304	47 574	37	159	.0239	1083	5.86
.101	178	40 281	26	146	.0201	999	5.88
-.008	140	37 905	28	143	.0189	943	5.10
.106	139	38 304	20	139	.0191	977	5.04
.204	224	43 543	28	144	.0218	1081	6.41
.297	329	49 051	31	153	.0246	1167	5.36
.408	437	55 815	29	162	.0282	1273	5.01
.509	487	59 977	25	165	.0304	1373	4.95
.602	567	67 010	14	169	.0341	1487	4.38
.698	607	74 384	9	165	.0380	1582	6.55
.812	774	70 906	17	94	.0362	1492	7.31
.880	1 559	47 929	1090	40	.0253	1199	5.74
.997	1 041	24 865	1995	20	.0138	721	8.38
Average	862	52 474	646	103	0.0240	----	------

TABLE A-III. - Concluded.

(c) Maximum afterburning power; engine inlet temperature T_2 = 245 K; engine inlet pressure Pt_2 = 2.20 N/cm^2; metered fuel-air FAABT = 0.058; exhaust nozzle radius R_8 = 39.15 cm; partial swirl augmentor.

R/R_8	COPPM	CO_2PPM	HCPPM	NO_xPPM	FAREMISS	TT_8, K	Pt_8, N/cm^2
-1.0	577	28 831	390	21	0.0147	961	3.05
0.909	779	62 550	24	56	.0319	1543	3.86
-.799	1 041	96 795	9	113	.0502	1847	1.39
.702	2 139	103 730	4	165	.0546	1895	3.45
-.615	1 503	102 660	3	195	.0536	1857	3.82
.500	1 197	100 900	3	205	.0525	1846	4.91
-.399	1 335	102 840	3	208	.0536	1865	5.85
.313	1 884	104 660	2	207	.0549	1888	5.91
-.215	2 739	104 600	4	202	.0554	1904	8.25
.111	3 166	104 600	3	196	.0556	1920	7.63
-.013	1 952	104 520	0	192	.0549	1932	6.60
.073	1 485	95 982	0	190	.0500	1881	5.93
.197	1 411	100 550	0	187	.0524	1929	8.17
.282	3 464	104 330	0	193	.0556	1925	7.46
.400	1 997	104 340	0	195	.0548	1895	9.01
.496	1 623	103 470	1	197	.0541	1879	8.85
.584	1 652	103 770	0	199	.0543	1876	8.67
.699	2 237	104 820	0	200	.0552	1884	8.94
.793	4 013	103 810	0	198	.0557	1904	8.80
.885	4 677	102 850	0	170	.0555	1927	8.05
1.0	1 836	102 970	0	138	.0540	1928	8.86
Average	2 113	93 650	11	161	0.0416	----	-----

TABLE A-IV. - ENGINE INLET CONDITIONS AND EXHAUST

PROFILE DATA FOR CONDITION 4

(a) Intermediate (nonafterburning) power; engine inlet temperature T_{2} = 243 K; engine inlet pressure Pt_{2} = 2.32 N/cm^{2}; metered fuel-air ratio FAABT = 0.013; exhaust nozzle radius R_{8} = 29.06 cm; Bill of Material augmentor.

R/R_{8}	COPPM	CO_{2}PPM	HCPPM	NO_{x}PPM	FAREMISS	TT_{8}, K	Pt_{8}, N/cm^{2}
-1.002	155	10 617	14	37	0.0052	494	6.62
-0.794	2 255	20 246	13	67	.0111	629	7.07
-.600	4 321	34 876	11	129	.0195	783	7.30
-.403	186	38 001	11	144	.0189	826	7.32
-.186	187	36 924	10	138	.0184	824	7.13
0.0	186	36 649	10	138	.0182	817	5.87
.199	187	37 561	5	140	.0187	826	7.18
.398	187	36 731	9	138	.0183	812	7.15
.608	189	31 529	9	132	.0157	744	7.10
.811	190	24 899	9	96	.0123	620	6.83
1.002	193	13 821	11	51	.0068	502	10.44
Average	954	26 179	10	97	0.0122	----	-----

TABLE A-IV. Continued.

(b) Partial afterburning power; engine inlet temperature T_2 = 244 K; engine inlet pressure Pt_2 = 2.22 N/cm^2; metered fuel-air ratio FAABT = 0.033; exhaust nozzle radius R_8 = 45.48 cm; calculated (adjusted) exhaust nozzle radius R_8^* = 38.77 cm; Bill of Material augmentor.

R/R_8	R/R_8^*	COPPM	CO_2PPM	HCPPM	NO_xPPM	FAREMISS	TT_8, K	Pt_8, N/cm^2
-0.999	------	201	889	8	10	0.0005	301	5.96
-.906	------	202	948	8	10	.0005	302	6.15
-.804	------	199	864	9	10	.0005	302	6.79
.706	-1.000	244	12 032	16	16	.0060	550	16.58
-.606	-.883	796	23 612	4331	23	.0142	995	10.27
.508	-.768	1647	50 808	1677	49	.0271	1339	12.19
-.404	-.646	771	74 410	8	133	.0381	1523	11.67
.296	-.520	284	60 972	40	160	.0308	1287	11.10
-.195	-.402	107	51 522	67	157	.0258	1083	10.58
.102	-.292	48	43 912	288	145	.0220	949	10.75
.002	-.171	20	39 171	1520	139	.0202	876	10.27
.103	-.052	11	38 267	2294	136	.0202	859	9.46
.194	.055	186	37 938	1303	136	.0196	856	8.69
.300	.181	34	40 078	1089	138	.0205	886	8.72
.402	.299	371	47 618	1351	144	.0246	985	8.58
.495	.408	676	58 703	535	155	.0301	1130	8.02
.594	.524	709	69 259	65	171	.0353	1314	7.75
.702	.651	598	79 304	20	172	.0406	1485	7.24
.796	.762	774	79 440	27	139	.0407	1460	6.94
.901	.884	953	59 667	269	77	.0306	1199	6.68
.999	1.06	450	29 476	467	36	.0150	766	9.19
Average	------	544	41 311	506	86	0.0189	-----	------

*Calculated (adjusted) data.

TABLE A-IV. Concluded.

(c) Maximum afterburning power; engine inlet temperature T_2 = 245 K; engine inlet pressure Pt_2 = 2.16 N/cm^2; metered fuel-air ratio FAABT = 0.059; exhaust nozzle radius R_8 = 48.76 cm; calculated (adjusted) exhaust nozzle radius R_8^* = 43.22 cm; Bill of Material augmentor.

R/R_8	R/R_8^*	COPPM	CO_2PPM	HCPPM	NO_xPPM	FAREMISS	TT_8, K	Pt_8, N/cm^2
-1.007	------	195	828	93	11	0.0005	297	7.01
0.902	------	194	2 452	62	11	.0013	349	6.69
-.807	-1.000	1 478	35 099	939	26	.0186	1002	9.00
.707	-0.890	1 441	80 827	36	66	.0418	1672	9.86
-.606	-.779	4 904	100 710	13	131	.0545	1827	10.35
.505	-.668	7 191	97 658	15	132	.0541	1796	10.42
-.403	-.555	3 883	101 220	8	187	.0542	1751	10.33
.305	-.447	4 560	101 040	8	181	.0541	1758	9.99
-.207	-.339	9 806	92 056	104	72	.0526	1753	9.61
.105	-.226	12 881	83 374	369	12	.0498	1739	10.53
0.00	-.116	10 180	91 206	46	11	.0524	1774	10.40
.093	.008	7 781	96 604	7	10	.0539	1804	10.52
.197	.107	9 685	92 629	8	10	.0528	1774	10.92
.297	.217	9 141	93 564	15	10	.0530	1764	10.70
.400	.330	1 914	99 147	5	157	.0519	1745	11.40
.501	.442	1 087	92 838	5	182	.0480	1702	10.99
.594	.544	1 315	95 901	4	194	.0498	1737	10.84
.697	.658	2 768	102 400	4	196	.0542	1796	10.29
.806	.777	1 870	99 896	4	164	.0523	1788	10.38
.895	.877	1 030	72 963	6	87	.0374	1492	8.66
1.007	1.000	284	16 922	13	24	.0084	649	10.79
Average	------	2 780	72 450	74	99	0.0331	----	------

*Calculated (adjusted) data.

TABLE A-V. - ENGINE INLET CONDITIONS AND EXHAUST

PROFILE DATA FOR CONDITION 5

[Mach 1.2 at 13.71 km (45 000 ft).]

(a) Intermediate (nonafterburning) power; engine inlet temperature T_{2} = 278 K; engine inlet pressure Pt_{2} = 3.51 N/cm^2; metered fuel-air ratio FAABT = 0.013; exhaust nozzle radius R_8 = 30.7[illegible] cm; partial swirl augmentor.

R/R_8	COPPM	CO_2PPM	HCPPM	NO_xPPM	FAREMISS	TT_8, K	Pt_8, N/cm^2
-1.013	262	19 481	6	90	0.0097	572	7.34
0.799	241	28 102	5	140	.0140	730	8.36
-.593	306	34 731	5	177	.0173	802	8.77
.391	282	37 641	4	191	.0188	845	9.27
-.220	262	38 807	1	192	.0194	867	8.86
.0196	314	38 431	2	186	.0192	864	5.85
.1956	268	39 005	1	189	.0195	866	9.10
.3972	326	37 626	1	181	.0188	837	9.35
.596	348	33 377	1	157	.0167	781	8.74
.802	307	24 391	0	43	.0121	666	8.26
1.0137	356	12 568	1	48	.0063	439	7.33
Average	273	28 302	2	122	0.0128	-----	-----

TABLE A-V. Continued.

(b) Partial afterburning power; engine inlet temperature T_2 = 278 K; engine inlet pressure Pt_2 = 3.47 N/cm^2; metered fuel-air ratio FAABT = 0.036; exhaust nozzle radius R_8 = 40.29 cm; partial swirl augmentor.

R/R_8	COPPM	CO_2PPM	HCPPM	NO_xPPM	FAREMISS	TT_8, K	Pt_8, N/cm^2
-1.00	201	27 003	279	17	0.0135	833	10.69
-.889	589	51 259	168	35	.0260	1299	7.50
-.785	387	72 769	12	107	.0370	1557	8.06
-.69	382	74 099	5	168	.0377	1573	8.23
-.598	277	66 565	5	192	.0337	1447	8.17
-.487	140	60 395	6	194	.0304	1332	8.18
-.398	90	57 238	7	192	.0287	1265	8.03
-.287	18	52 686	8	191	.0263	1173	7.85
-.198	184	46 760	8	184	.0234	1090	7.48
.087	195	39 435	2	172	.0197	981	5.95
.0	202	38 295	3	168	.0191	931	2.57
.119	195	39 778	2	171	.0198	1001	6.62
.204	186	45 141	7	181	.0226	1082	7.18
.291	11	52 035	8	188	.0260	1190	7.28
.410	70	57 274	7	192	.0287	1275	7.46
.513	128	61 802	6	193	.0311	1367	7.65
.609	230	69 718	2	191	.0353	1499	7.77
.692	302	80 607	1	176	.0411	1642	7.86
.810	236	83 628	1	108	.0426	1599	7.78
.895	581	57 210	115	34	.0290	1274	7.16
1.00	366	28 396	689	11	.0145	697	5.48
Average	301	60 002	53	129	0.0267	----	-----

TABLE A-V. Concluded.

(c) Maximum afterburning power; engine inlet temperature T_{t_2} = 278 K; engine inlet pressure Pt_2 = 3.55 N/cm^2; metered fuel-air ratio FAABT = 0.066; exhaust nozzle radius R_8 = 46.99 cm; partial swirl augmentor.

R/R_8	COPPM	CO_2PPM	HCPPM	NO_xPPM	FAREMISS	TT_8, K	Pt_8, N/cm^2
-1.00	814	37 907	156	18	0.0193	1176	5.88
0.920	750	89 799	15	68	.0462	1826	7.26
-.801	14 402	79 679	1465	3	.0493	1882	7.32
.705	13 085	84 980	964	1	.0512	1845	7.19
-.610	6 579	101 210	25	1	.0557	1871	7.38
.520	4 073	104 510	6	1	.0561	1898	7.30
-.421	6 145	101 690	5	1	.0557	1980	7.28
.300	7 338	99 415	4	1	.0552	1867	7.03
-.205	6 442	101 110	4	1	.0556	1868	6.31
.110	1 732	103 320	4	1	.0541	1844	5.42
.0192	838	92 974	4	184	.0480	1801	4.94
.101	2 137	104 260	3	200	.0548	1872	5.56
.195	6 539	100 940	3	181	.0556	1878	6.60
.289	5 551	102 640	3	1	.0559	1875	7.02
.389	4 814	103 540	3	1	.0560	1881	7.23
.477	7 029	100 000	10	1	.0553	1870	7.57
.597	11 501	90 377	119	1	.0527	1852	7.79
.693	13 624	82 845	401	1	.0500	1854	7.93
.788	13 377	83 993	334	1	.0504	1889	7.81
.887	912	95 476	3	76	.0494	1818	7.34
.983	984	46 164	47	30	.0235	1018	7.52
Average	6 716	88 602	237	24	0.0417	----	-----

TABLE A-VI. - ENGINE INLET CONDITIONS AND EXHAUST

PROFILE DATA FOR CONDITION 6

[Mach 1.2 at 13.71 km (45 000 ft).]

(a) Intermediate (nonafterburning) power; engine inlet temperature T_2 = 278 K; engine inlet pressure Pt_2 = 3.55 N/cm^2; metered fuel-air ratio FAABT = 0.013; exhaust nozzle radius R_8 = 31.93 cm; Bill of Material augmentor.

R/R_8	COPPM	CO_2PPM	HCPPM	NO_xPPM	FAREMISS	TT_8, K	Pt_8, N/cm^2
-1.00	219	4 843	2	33	0.0024	479	8.25
-0.811	222	12 949	1	76	.0064	570	7.92
-.607	200	31 051	1	198	.0154	766	8.47
.403	211	39 677	0	260	.0198	849	9.62
-.205	223	38 597	0	248	.0192	849	9.69
0.0	210	38 267	3	244	.0191	848	6.35
.195	211	39 285	3	245	.0196	861	9.60
.390	228	39 469	3	246	.0197	852	9.58
.595	240	35 779	3	234	.0178	794	8.59
.798	226	28 425	3	181	.0141	677	8.30
.995	247	15 109	3	87	.0075	536	12.26
Average	208	25 835	2	164	0.0117	----	------

TABLE A-VI. Continued.

(b) Partial afterburning power; engine inlet temperature T_2 = 278 K; engine inlet pressure Pt_2 = 3.48 N/cm^2; metered fuel-air ratio FAABT = 0.033; exhaust nozzle radius R_8 = 39.2 cm; Bill of Material augmentor.

R/R_8	COPPM	CO_2PPM	HCPPM	NO_xPPM	FAREMISS	TT_8, K	Pt_8, N/cm^2
-1.021	526	20 069	2997	21	0.0116	912	6.54
0.934	993	34 928	2992	33	.0193	1226	7.07
-.832	873	63 818	125	91	.0326	1382	7.77
.732	415	78 657	21	205	.0401	1617	7.95
-.631	259	65 678	13	252	.0332	1394	8.11
.518	107	53 644	20	260	.0269	1164	8.16
-.429	67	48 120	32	254	.0240	1051	8.19
.328	65	44 016	108	240	.0220	971	8.15
-.229	129	42 467	323	230	.0213	941	8.29
.130	166	42 355	580	226	.0214	941	8.44
-.031	118	41 241	497	225	.0218	908	5.79
.072	96	41 996	393	230	.0211	927	8.39
.171	126	46 197	183	239	.0232	976	8.23
.270	155	53 799	48	254	.0270	1068	8.23
.370	165	61 478	10	269	.0310	1194	8.23
.478	213	68 089	5	277	.0344	1332	8.21
.575	252	75 665	10	280	.0384	1474	8.10
.673	313	86 568	10	276	.0443	1620	8.09
.774	395	83 758	16	202	.0428	1541	7.72
.871	615	62 426	102	113	.0317	1259	7.92
1.020	282	27 522	347	42	.0129	621	2.41
Average	406	58 804	467	182	0.0264	-----	-----

TABLE A-VI. Concluded.

(c) Maximum afterburning power; engine inlet temperature T_2 = 277 K; engine inlet pressure Pt_2 = 3.50 N/cm^2; metered fuel-air ratio FAABT = 0.064; exhaust nozzle radius R_8 = 46.4 cm; Bill of Material augmentor.

R/R_8	COPPM	CO_2PPM	HCPPM	NO_xPPM	FAREMISS	TT_8, K	Pt_8, N/cm^2
-1.044	1 052	36 671	205	29	0.0188	900	7.48
-0.907	1 208	99 624	11	106	.0518	1831	7.59
-.836	12 595	86 846	470	10	.0516	1862	7.93
-.634	13 535	83 033	811	8	.0503	1814	8.13
-.423	6 372	101 140	15	8	.0556	1837	7.75
-.347	10 406	92 794	109	8	.0534	1836	7.64
-.135	10 879	91 045	31	8	.0527	1836	6.15
.069	10 180	92 847	37	8	.0532	1805	6.11
.269	9 076	96 422	35	8	.0546	1787	7.53
.506	3 309	105 170	12	8	.0560	1817	7.95
.608	10 381	92 924	79	9	.0534	1833	8.07
.766	12 768	85 583	147	9	.0508	1853	7.89
.904	705	77 577	12	106	.0397	1595	7.31
1.044	1 093	34 978	335	44	.0180	718	2.48

APPENDIX B

SYMBOLS

COPPM	Carbon monoxide concentration, ppmv
CO_2PPM	Carbon dioxide concentration, ppmv
F/A	Overall afterburner fuel air-ratio
FAABT	Metered fuel-air ratio
FAREMISS	Fuel-air ratio calculated from gas samples
HCPPM	Hydrocarbon concentration, ppmC
NO_xPPM	Oxides of nitrogen concentration, ppmv
Pt_2	Engine inlet pressure, N/cm^2
Pt_8	Exhaust total pressure, N/cm^2
R	Radius, cm
R_8	Exhaust nozzle radius, cm
T_2	Engine inlet temperature, K
Tt_8	Exhaust total temperature, K

REFERENCES

1. Moss, John E., Jr.; Cullom, Richard R.: Exhaust Emission Survey of an F100 Afterburning Turbofan Engine at Simulated Flight Altitude Conditions. NASA TM-81656, 1981.

2. Diehl, Larry A.: Preliminary Investigation of Gaseous Emissions from Jet Engine Afterburners. NASA TM X-2323, 1971.

3. Palcza, J. Lawrence: Study of Altitude and Mach Number Effects on Exnaust Gas Emissions of an Afterburning Turbofan Engine. NAPTC-ATD-212, Naval Air Propulsion Test Center, 1971. (AD-741249; FAA-RD-72-31)

4. Dienl, Larry A.: Measurement of Gaseous Emissions from an Afterburning Turbojet Engine at Simulated Altitude Conditions. NASA TM X-2726, 1973.

5. German, R.C.; High, M.D.; and Robinson, C.E.: Measurement of Exhaust Emissions from a J85-GE-5B Engine at Simulated High-Altitude Supersonic Free-Stream Flight Conditions. ARO-PWT-TR-73-49, ARO, Inc., 1973. (AD-764-717; AEDC-TR-73-103; FAA RD-73-92)

6. Davidson, D.L.; and Domal, A.F.: Emission Measurements of a J93 Turbojet Engine. ARO-ETF-TR-73-46, ARO, Inc., 1973. (AD-766648; AEDC-TR-73-132)

7. Holdeman, James D.: Exhaust Emission Calibration of Two J-58 Afterburning Turbojet Engines at Simulated High Altitude, Supersonic Flight Conditions. NASA TN D-8173, 1976.

8. Taylor, J. W. R., ed.: Jane's All the World's Aircraft, 1979-80. Pratt and Whitney JTF22 (F100). Jane's Publishing, Inc., New York, 1979, pp. 757-758.

9. Procedure for the Continuous Sampling and Measurement of Gaseous Emissions from Aircraft Turbine Engines. Aerospace Recommended Practice 1256, Society of Automotive Engineers, Oct. 1971.

TABLE I. – TEST CONDITIONS

Test condition	Simulated Mach number	Simulated altitude		Overall metered fuel-air ratio, FAAPT	Engine inlet pressure, Pt_2		Engine inlet temperature, T_2		Primary combustor pressure		Afterburner mixed inlet pressure		Afterburner mixed inlet temperature		Augmentor configuration
		km	ft		N/cm^2	psia	K	°R	N/cm^2	psia	N/cm^2	psia	K	°R	
1	0.8	10.97	36 000	0.062	2.69	3.96	244	440	93	135	10.9	15.83	722	1299	Swirl
2	.8	10.97	36 000	.012	3.37	4.89	245	442	89.5	130	10.7	15.52	709	1276	Bill of Material
2	.8	10.97	36 000	.061	3.43	4.98	245	441	90.7	132	10.8	15.68	720	1296	Bill of Material
3	0.8	13.71	45 000	0.013	2.22	3.23	242	436	60.4	88	7.0	10.14	702	1264	Swirl
3	.8	13.71	45 000	.033	2.19	3.18	240	432	60.3	87	7.0	10.14	705	1269	Swirl
3	.8	13.71	45 000	.058	2.20	3.20	245	440	60.4	88	7.0	10.14	723	1301	Swirl
4	0.8	13.71	45 000	0.013	2.32	3.37	243	438	61.4	89	7.2	10.43	706	1270	Bill of Material
4	.8	13.71	45 000	.033	2.22	3.23	244	439	60.2	87	7.1	10.24	710	1277	Bill of Material
4	.8	13.71	45 000	.059	2.16	3.13	245	441	58.9	86	6.9	10.03	724	1304	Bill of Material
5	1.2	13.71	45 000	0.013	3.51	5.10	278	501	86.2	125	10.42	15.11	764	1375	Swirl
5	1.2	13.71	45 000	.036	3.47	5.04	278	502	84.8	123	10.38	15.05	773	1392	Swirl
5	1.2	13.71	45 000	.066	3.55	5.16	278	501	88.0	128	10.69	15.51	770	1385	Swirl
6	1.2	13.71	45 000	0.013	3.55	5.15	278	502	83.9	122	10.37	15.04	752	1356	Bill of Material
6	1.2	13.71	45 000	.033	3.48	5.06	278	501	83.1	121	10.28	15.06	766	1380	Bill of Material
6	1.2	13.71	45 000	.064	3.50	5.08	277	498	83.7	121	10.42	15.11	770	1386	Bill of Material

TABLE II. – COMBUSTION EFFICIENCIES (WITH AND WITHOUT AFTERBURNING)

Simulated Mach number	Simulated altitude		Power level	Augmentor configuration	Combustion efficiency	Afterburner mixed inlet pressure	
	km	ft				N/cm^2	psia
0.8	10.97	36 000	Maximum afterburning	Swirl	98	10.9	15.82
.8	10.97	36 000	Intermediate	Bill of Material	99	10.7	15.52
.8	10.97	36 000	Maximum afterburning	Bill of Material	97	10.8	15.68
0.8	13.71	45 000	Intermediate	Swirl	—	7.0	10.14
.8	13.71	45 000	Partial afterburning	Swirl	97	7.0	10.14
.8	13.71	45 000	Maximum afterburning	Swirl	98	7.0	10.14
0.8	13.71	45 000	Intermediate	Bill of Material	98	7.2	10.43
.8	13.71	45 000	Partial afterburning	Bill of Material	98	7.1	10.24
.8	13.71	45 000	Maximum afterburning	Bill of Material	98	6.9	10.03
1.2	13.71	45 000	Intermediate	Swirl	99	10.42	15.11
1.2	13.71	45 000	Partial afterburning	Swirl	99	10.33	15.05
1.2	13.71	45 000	Maximum afterburning	Swirl	96	10.69	15.51
1.2	13.71	45 000	Intermediate	Bill of Material	99	10.37	15.04
1.2	13.71	45 000	Partial afterburning	Bill of Material	98	10.38	15.06
1.2	13.71	45 000	Maximum afterburning	Bill of Material	—	10.42	15.11

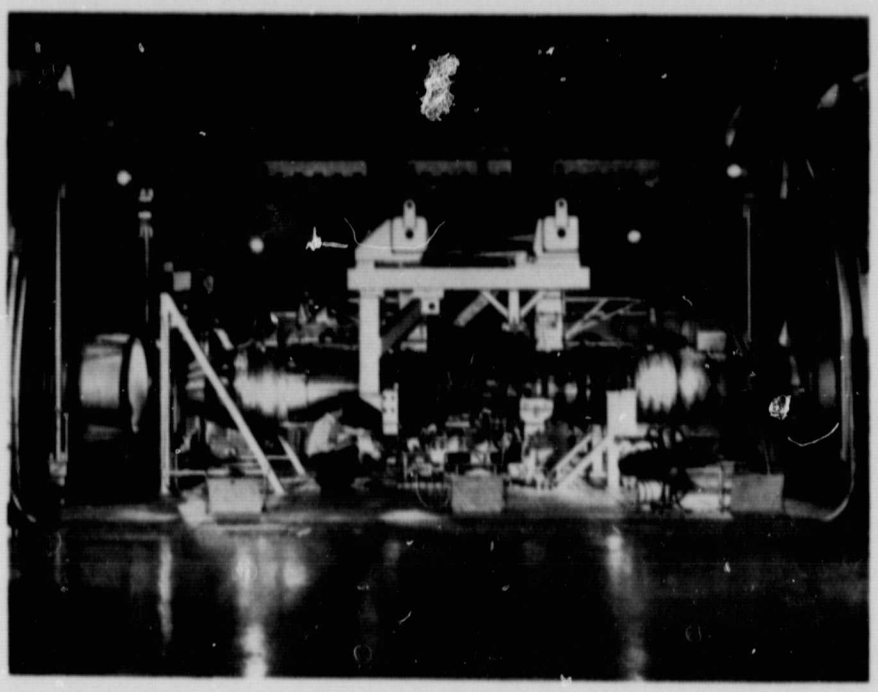

Figure 1. - Afterburning turbofan engine installed in altitude test chamber.

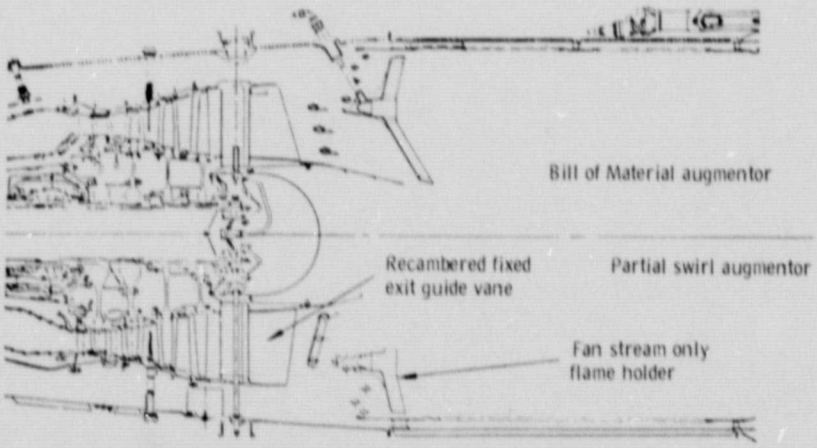

(a) Sketch of partial swirl and Bill of Material augmentors.

Figure 2. - Partial swirl and Bill of Material augmentors.

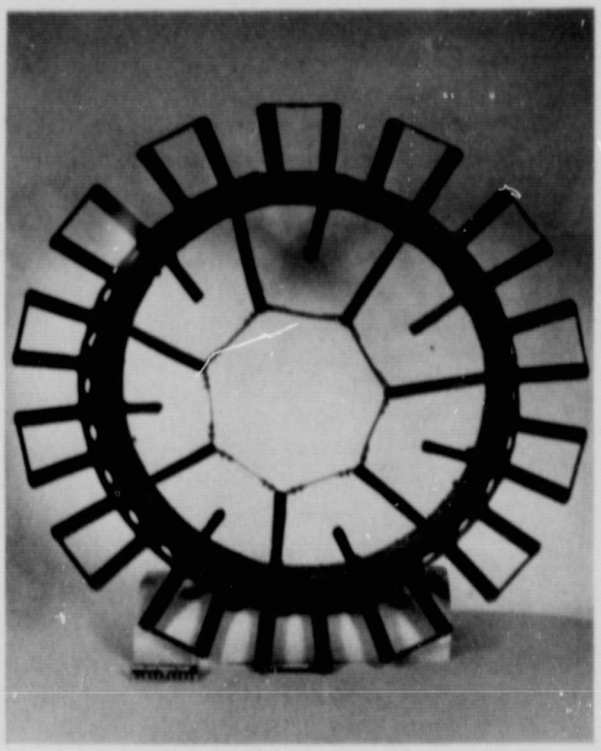

(b) Bill of material flame holder.

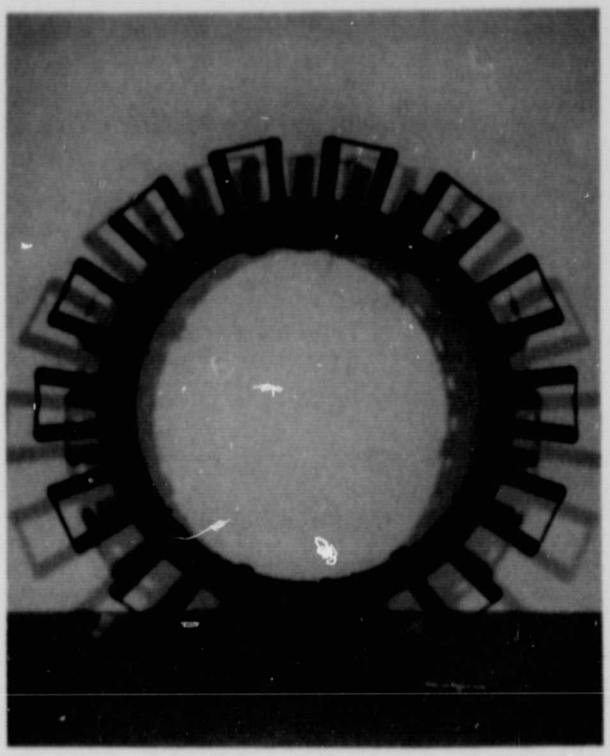

(c) Partial swirl flame holder.

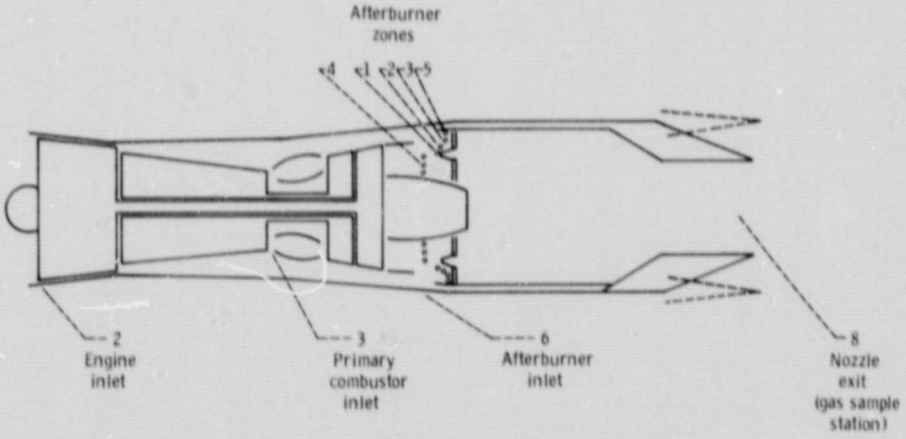

(d) Engine instrumentation location.

Figure 2. - Concluded.

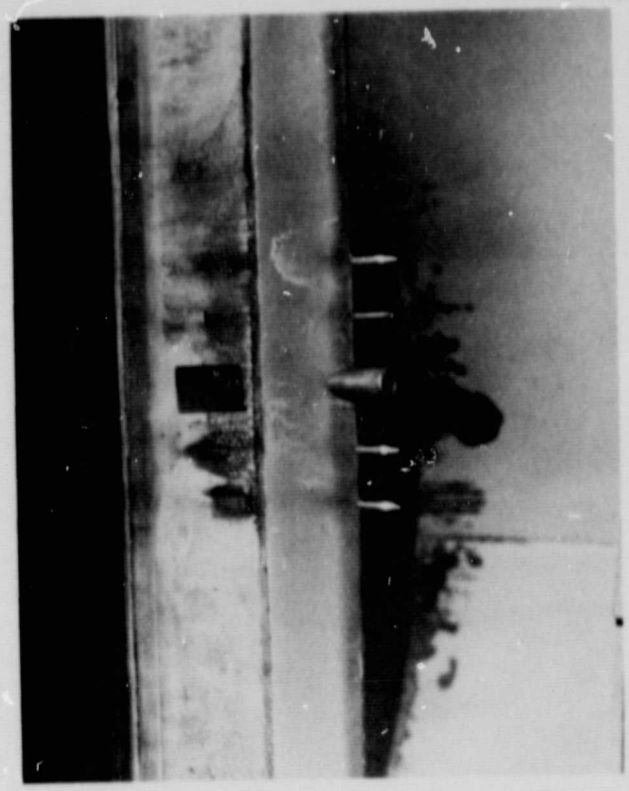

(a) Detail of sensor area.

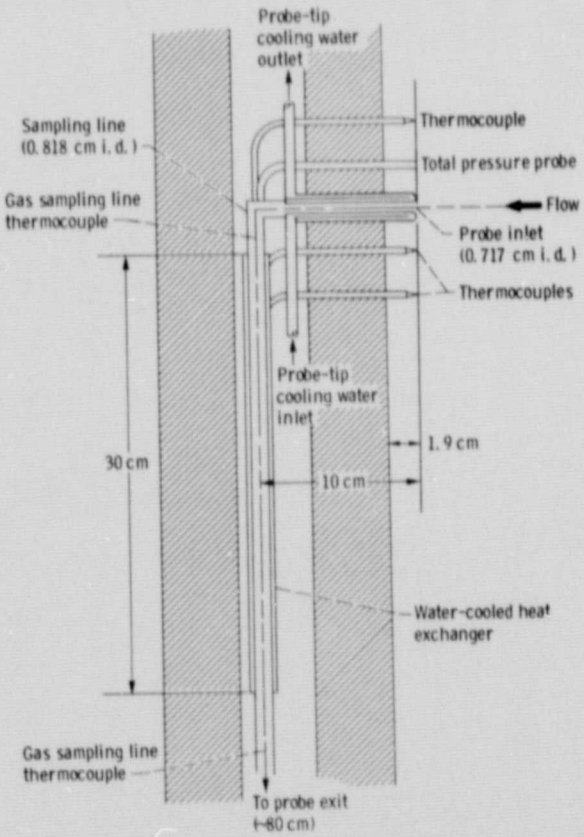

(b) Schematic of gas sample probe.

Figure 3. - Sensor area of probe.

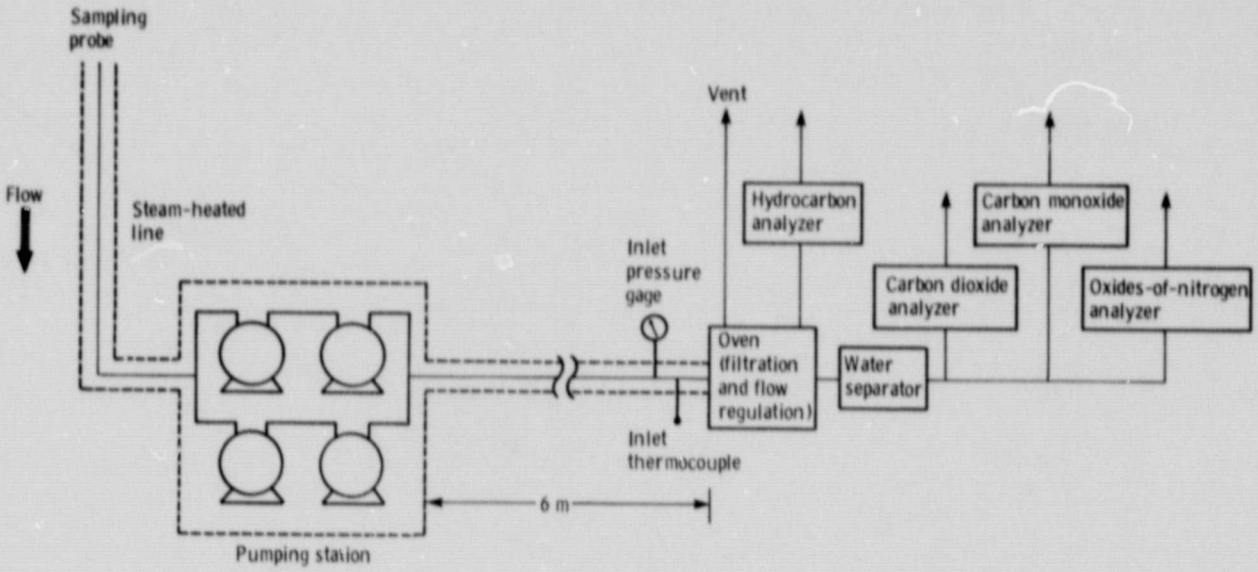

(a) Flow schematic.

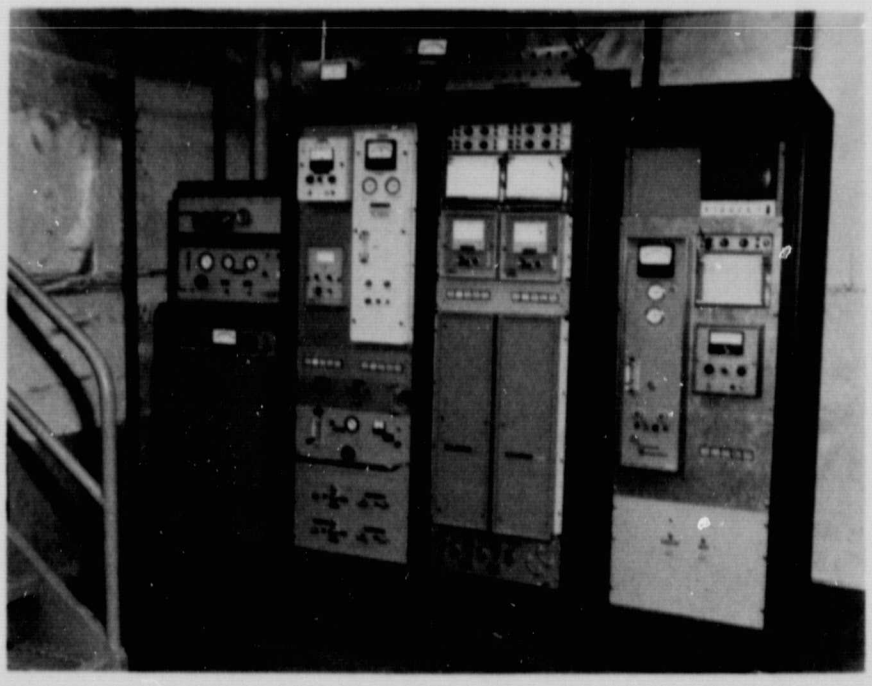

(b) Console.

Figure 4. - Gas analysis system.

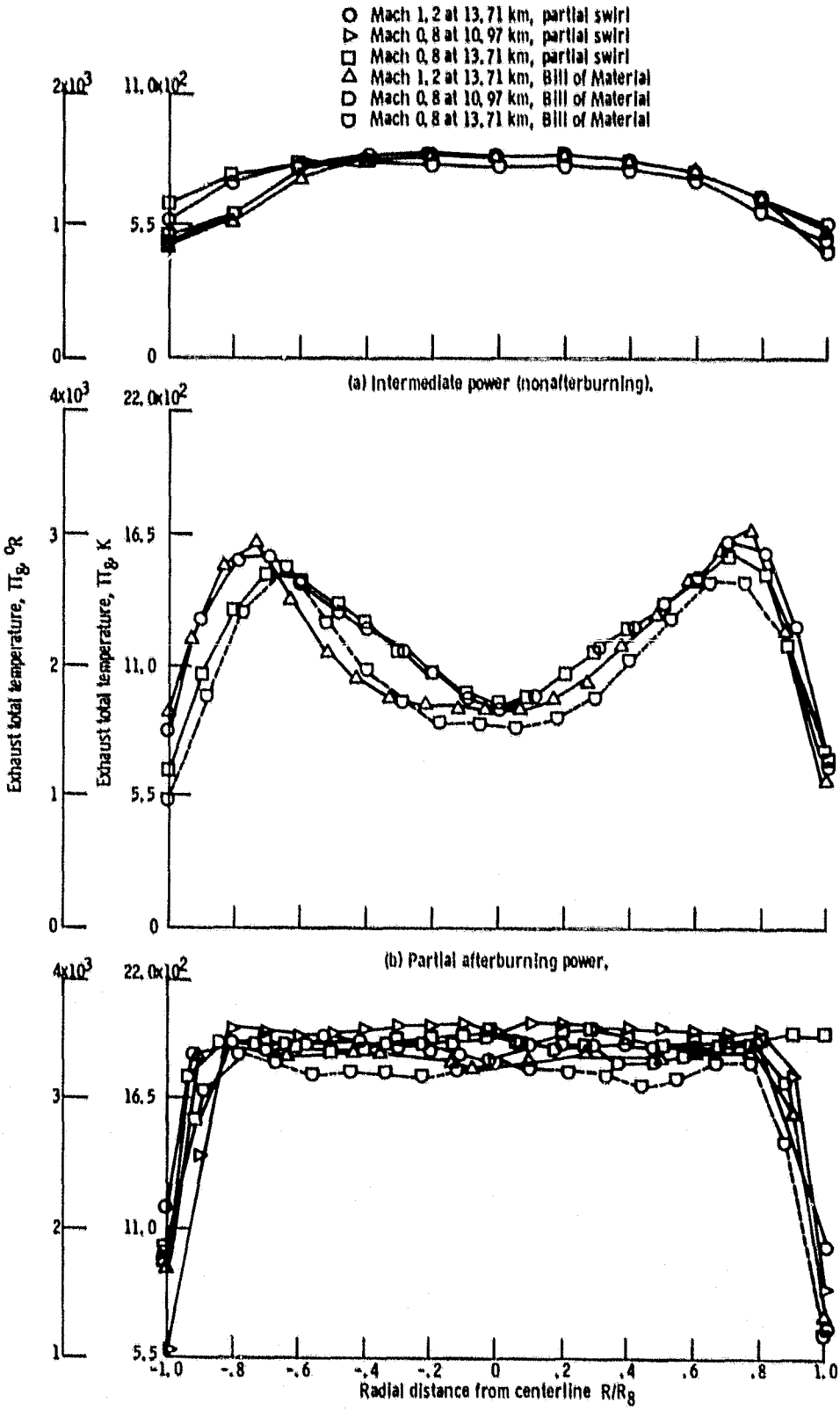

Figure 5. - Total temperature distribution.

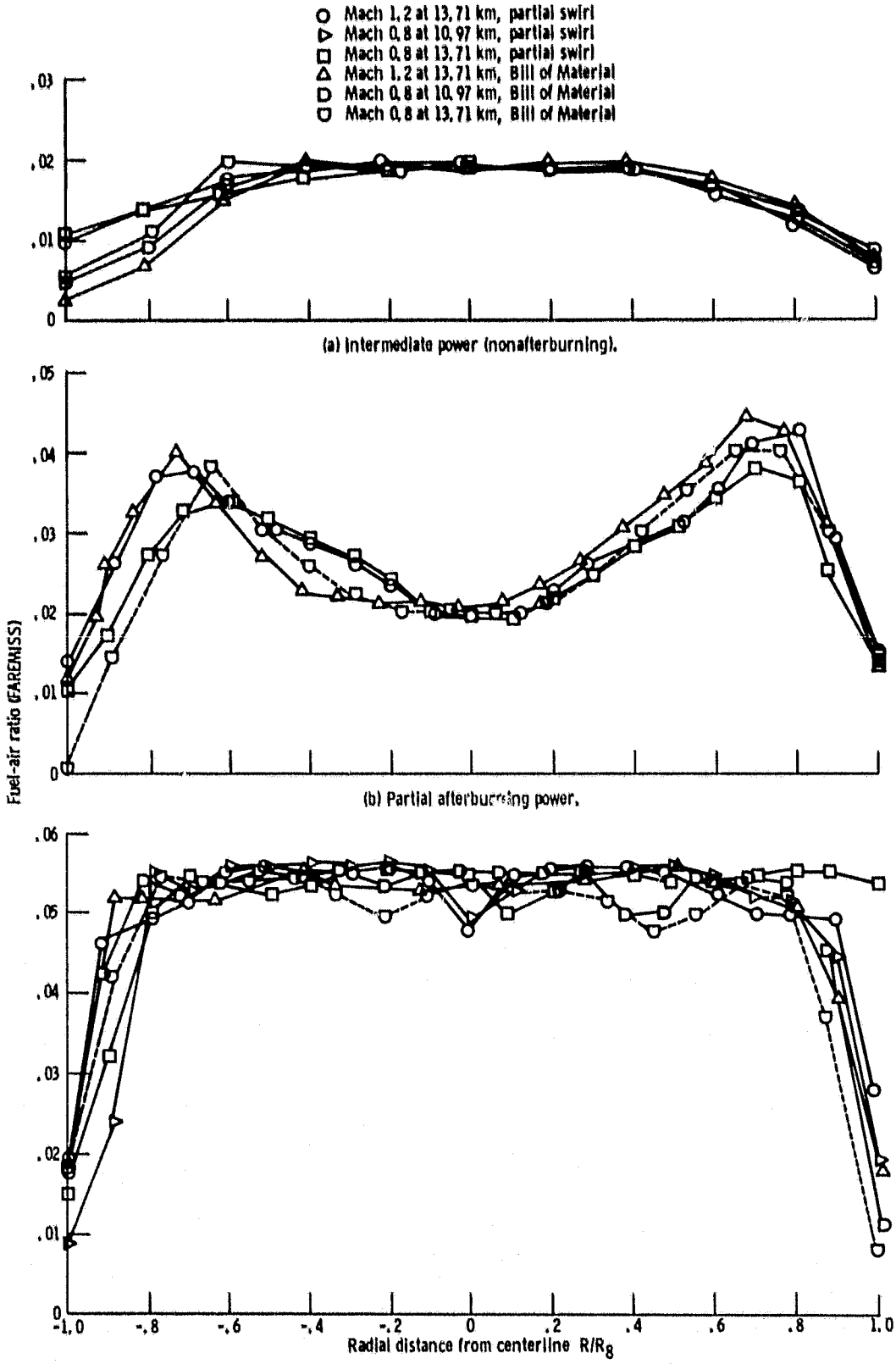

Figure 6. - Local fuel-air ratio (FAREMISS) profile.

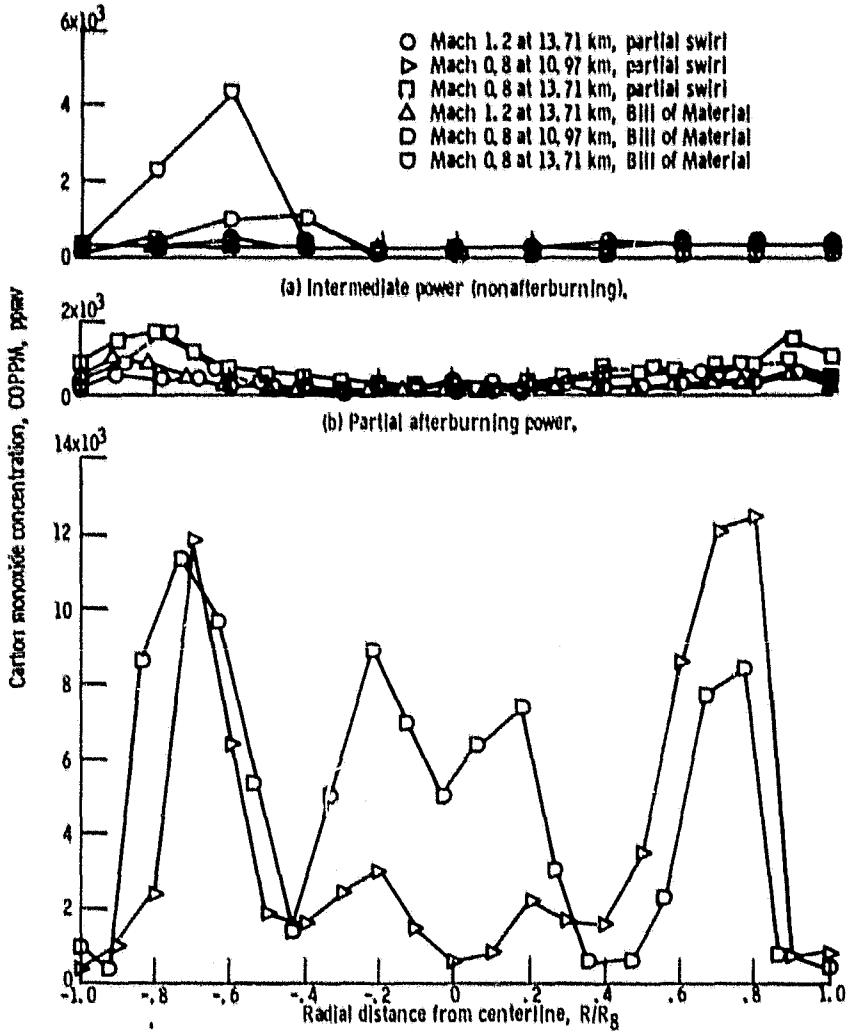

(a) Intermediate power (nonafterburning).

(b) Partial afterburning power.

(c) Maximum afterburning power, Mach 0.8 at 10.97 km.

Figure 7. - Carbon monoxide concentration profile.

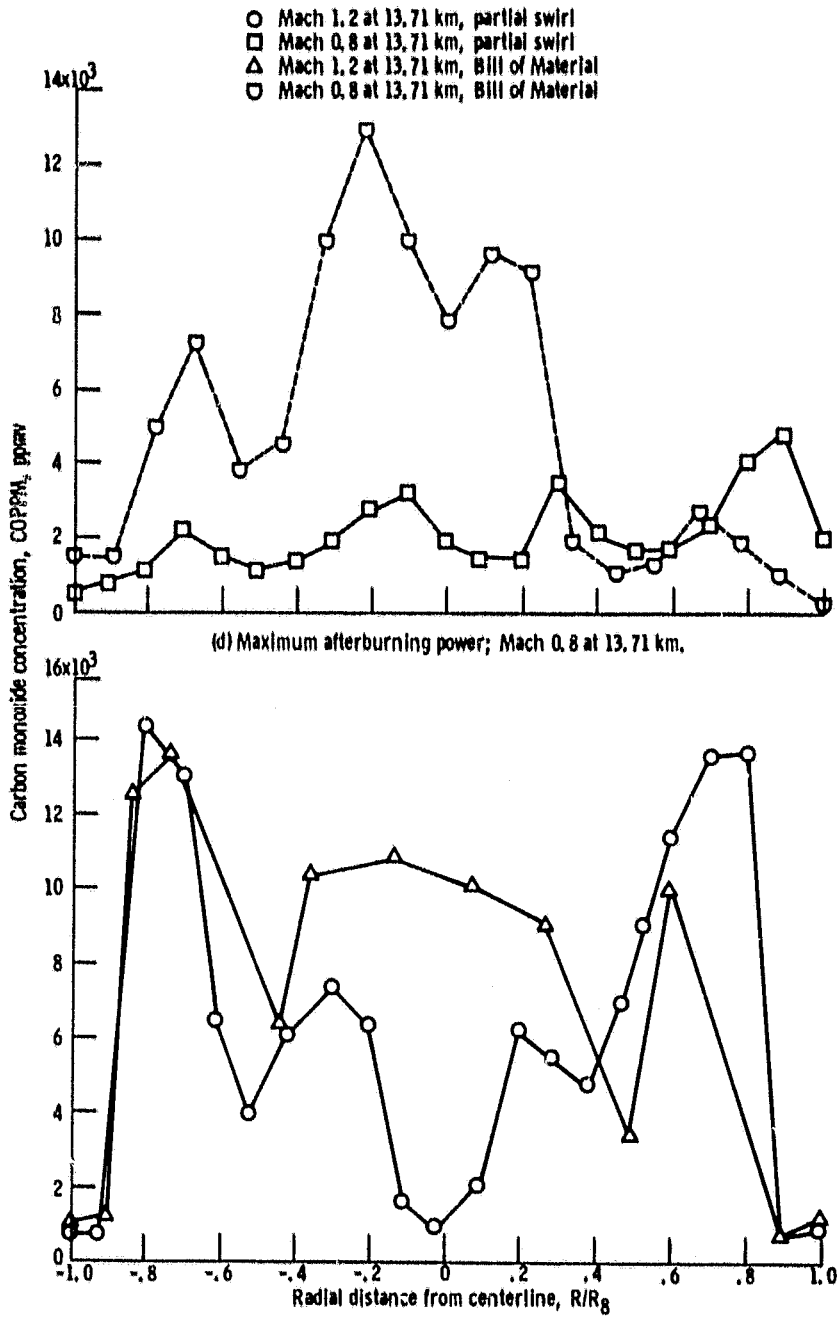

(d) Maximum afterburning power; Mach 0.8 at 13.71 km.

(e) Maximum afterburning power; Mach 1.2 at 13.71 km.

Figure 7. - Concluded.

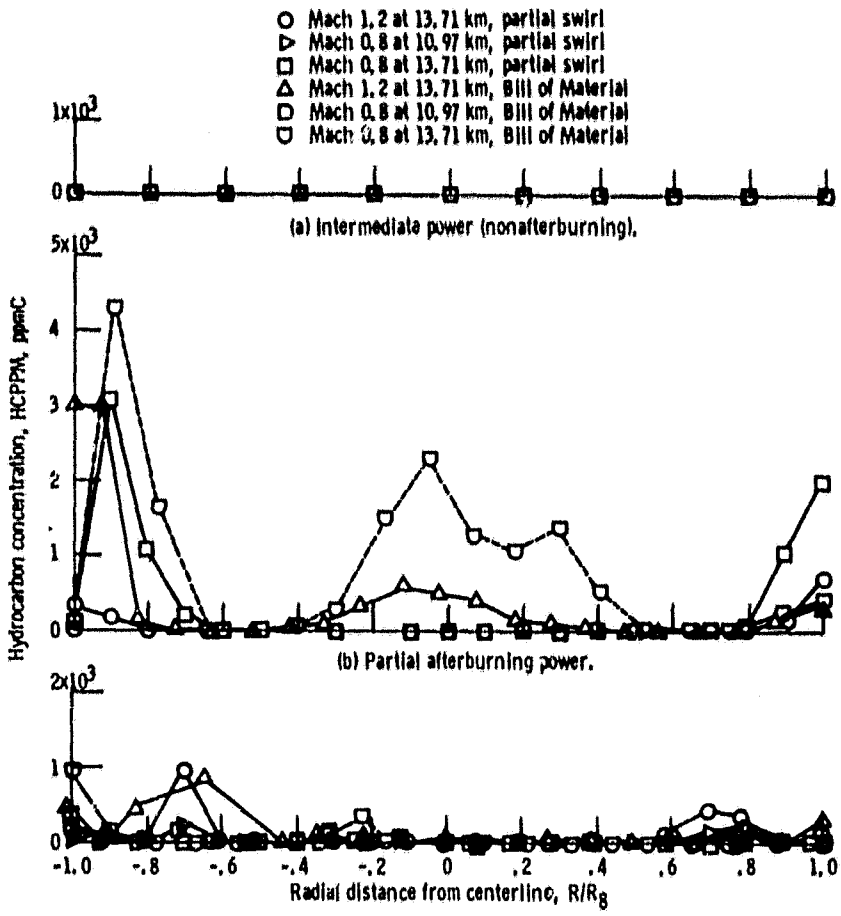

Figure 8. - Hydrocarbon concentration profiles.

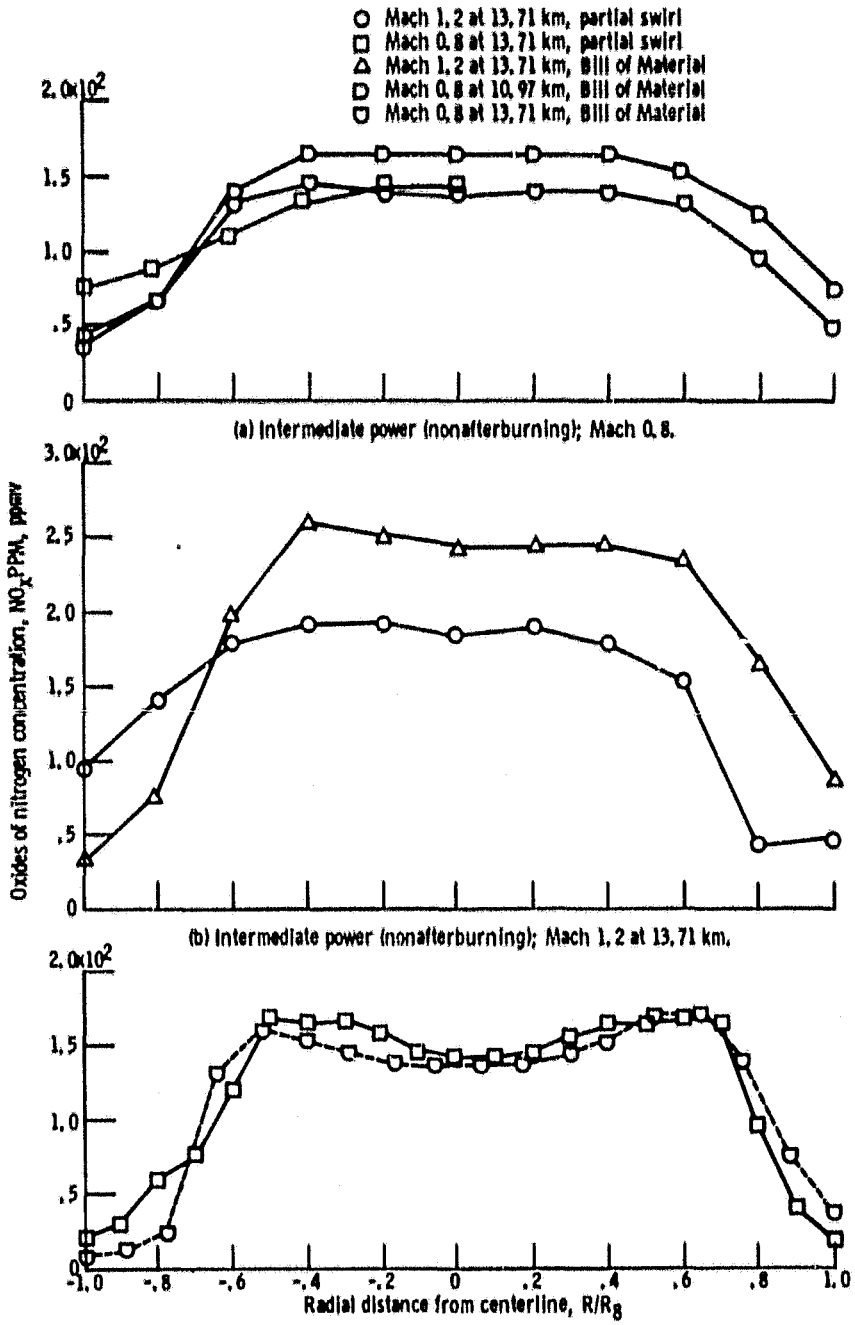

(a) Intermediate power (nonafterburning); Mach 0.8.

(b) Intermediate power (nonafterburning); Mach 1.2 at 13.71 km.

(c) Partial afterburning power; Mach 0.8 at 13.71 km.

Figure 9. - Oxides of nitrogen concentration profiles.

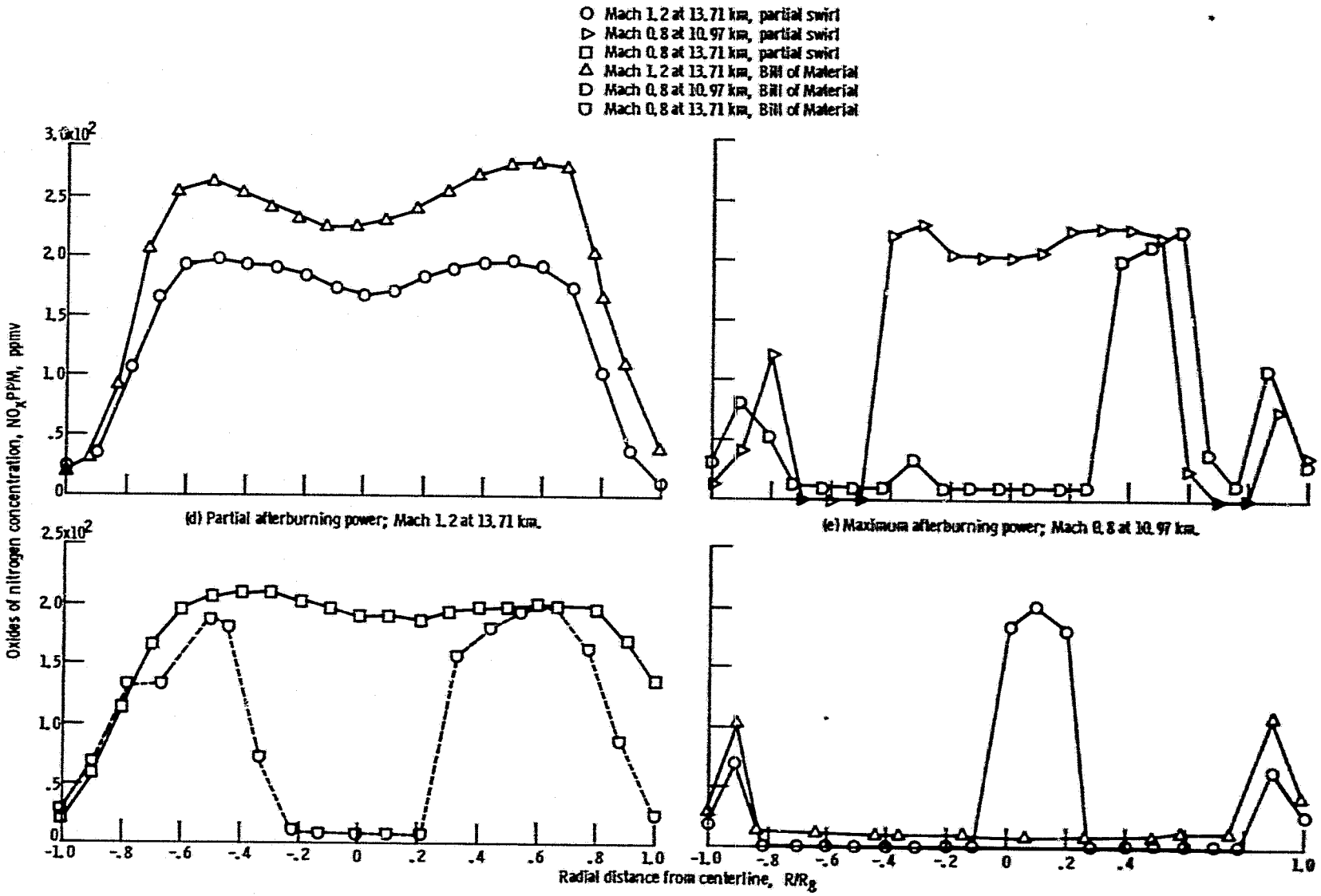

(d) Partial afterburning power; Mach 1.2 at 13.71 km.

(e) Maximum afterburning power; Mach 0.8 at 10.97 km.

(f) Maximum afterburning power; Mach 0.8 at 13.71 km.

(g) Maximum afterburning power; Mach 1.2 at 13.71 km.

Figure 9. – Concluded.

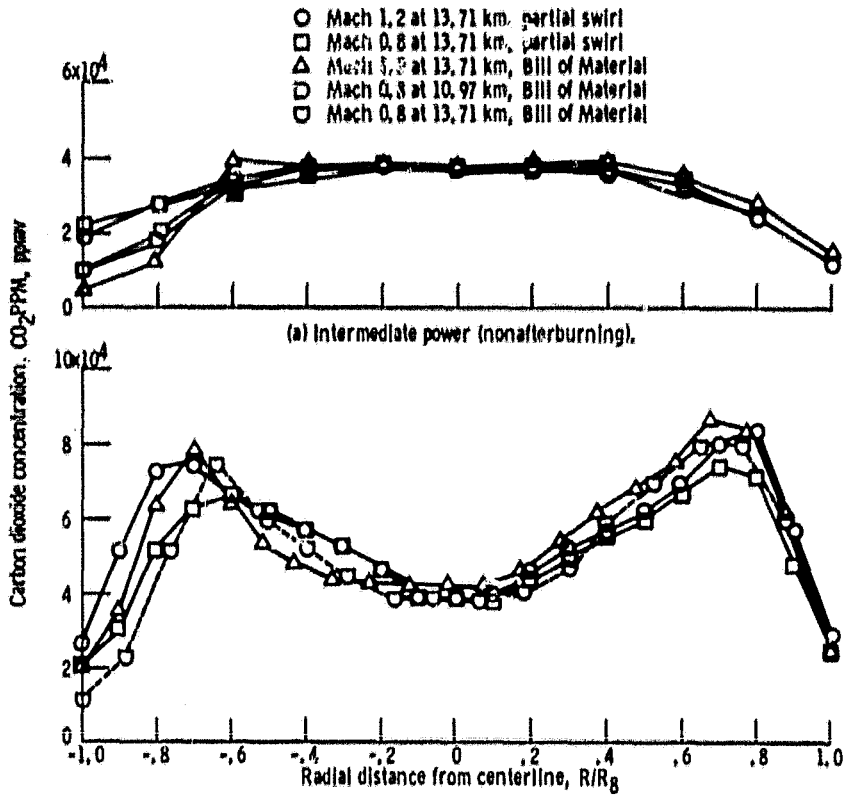

(a) Intermediate power (nonafterburning).

(b) Partial afterburning power.

Figure 10. - Carbon dioxide concentration.

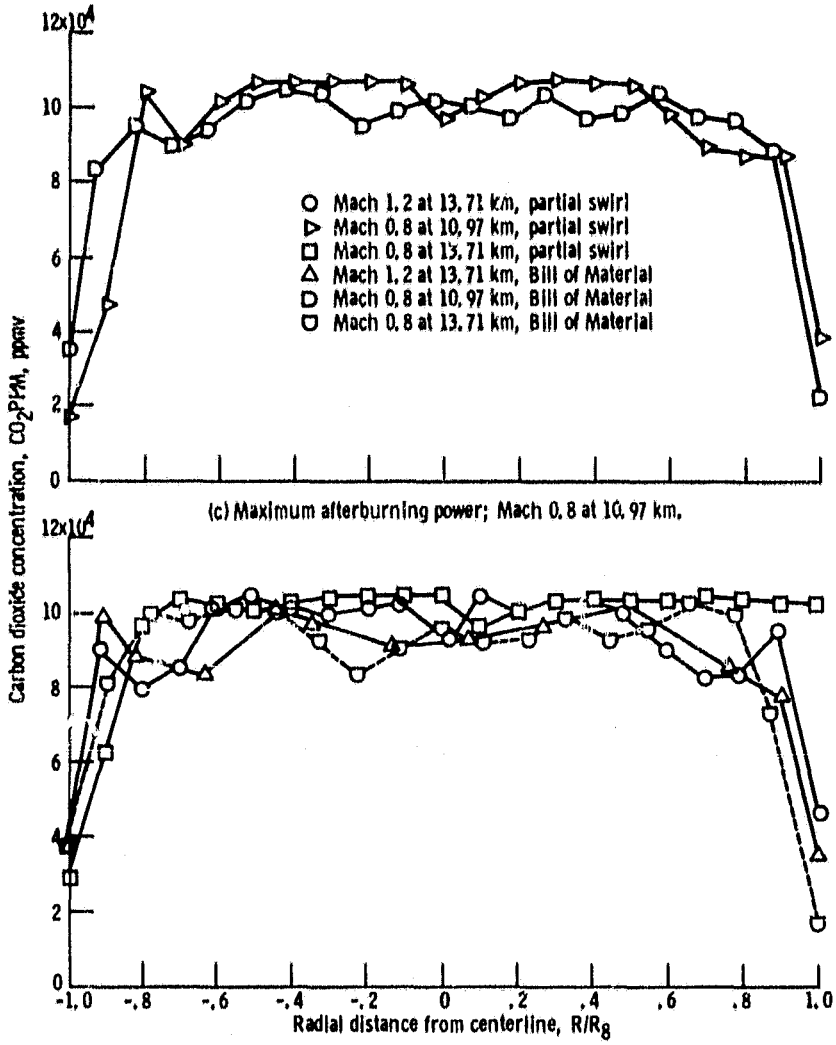

(c) Maximum afterburning power; Mach 0.8 at 10.97 km.

(d) Maximum afterburning power; 13.71 km.

Figure 10. - Concluded.

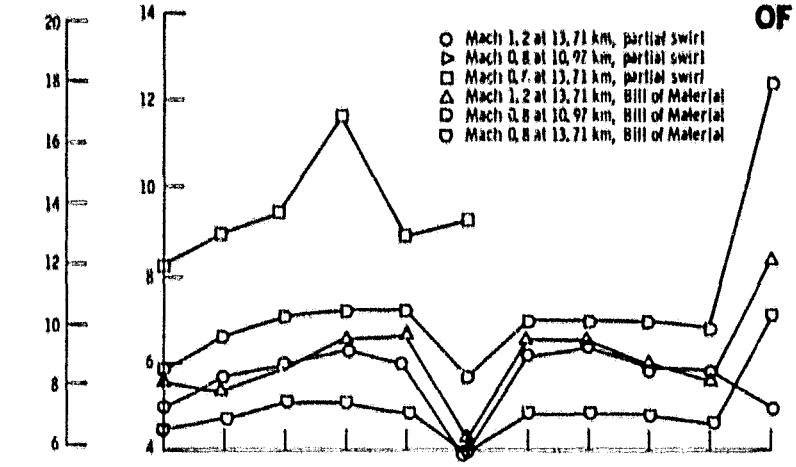

(a) Intermediate power (nonafterburning).

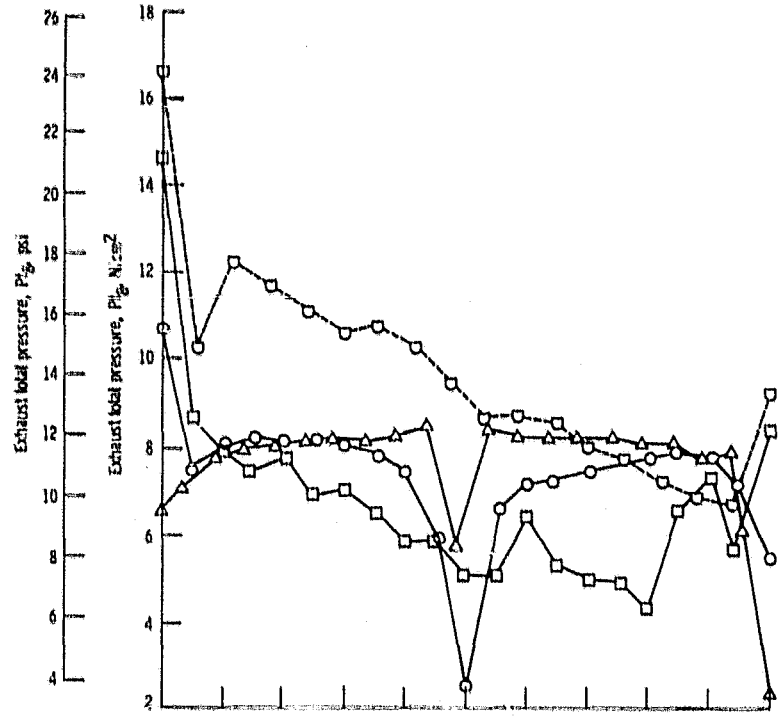

(b) Partial afterburning power.

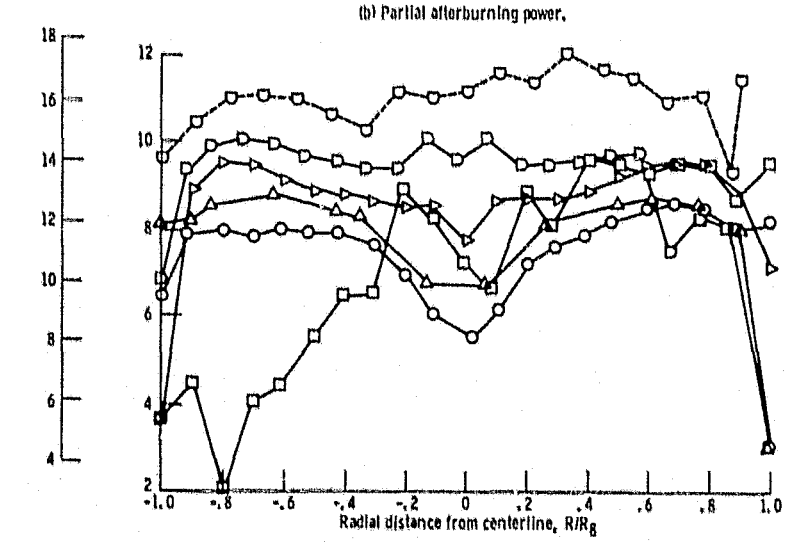

(c) Maximum afterburning power.

Figure 11. - Exhaust total pressure profile.

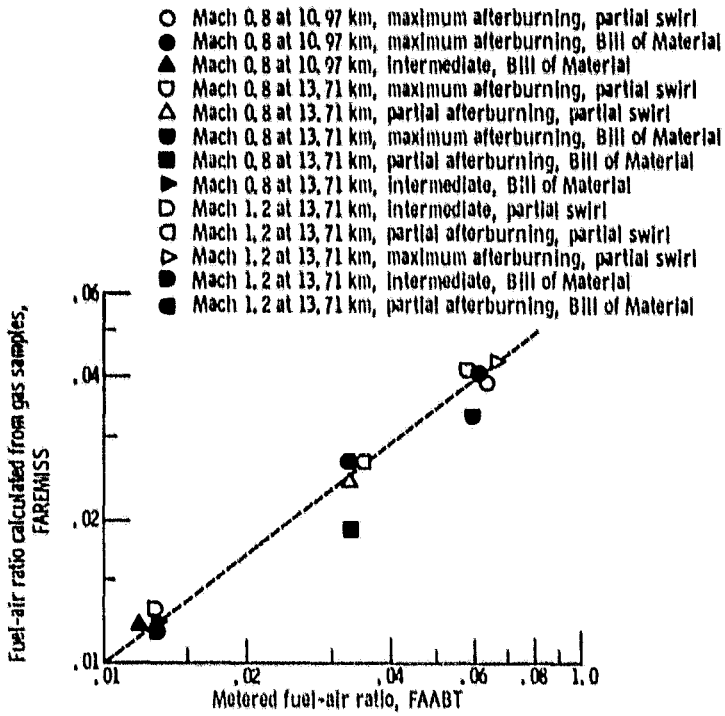

Figure 12. - Comparison of gas sample and metered fuel-air ratio.

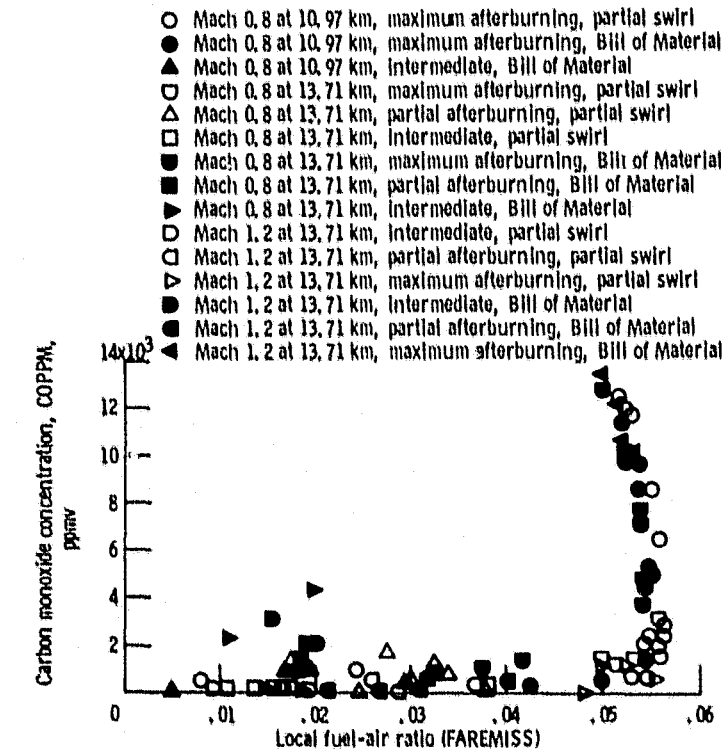

Figure 13. - Variation of carbon monoxide with gas sample fuel-air ratio.

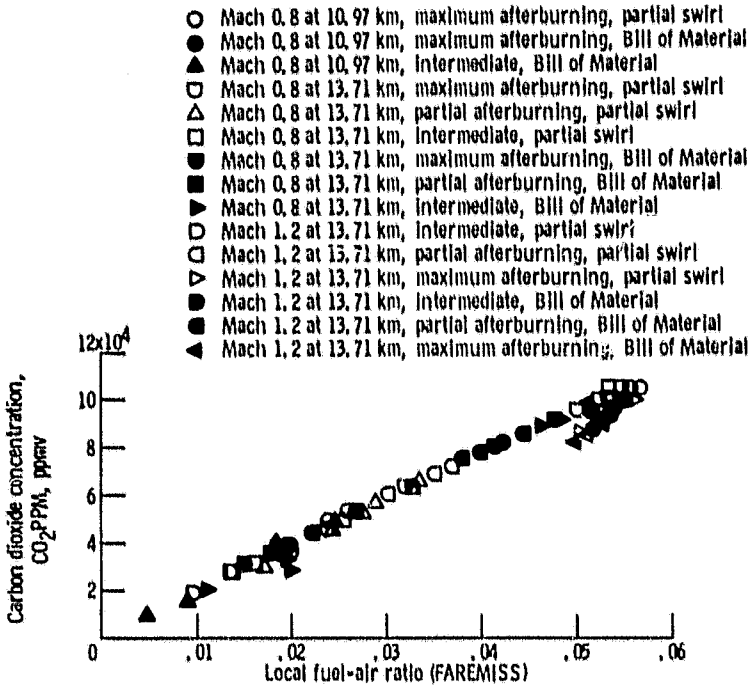

Figure 14. - Variation of carbon dioxide with gas sample fuel-air ratio.

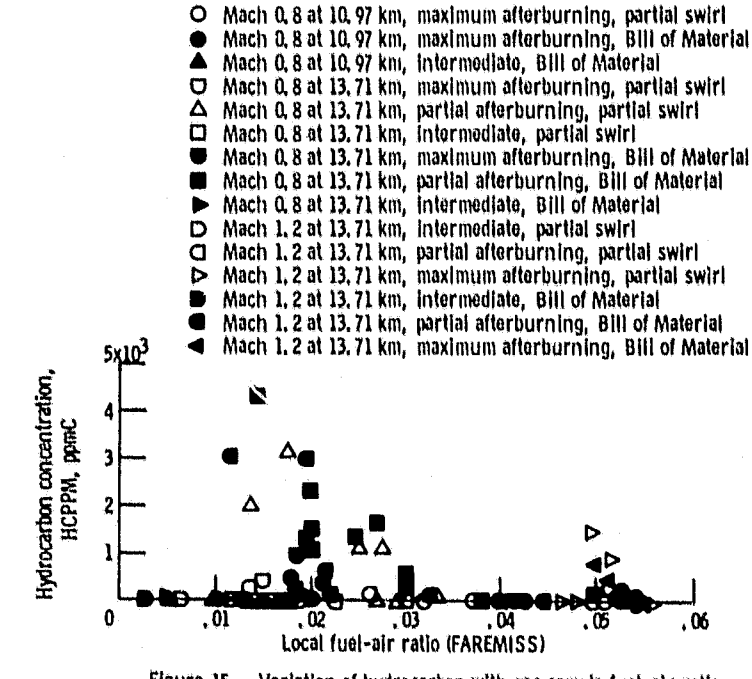

Figure 15. - Variation of hydrocarbon with gas sample fuel-air ratio.

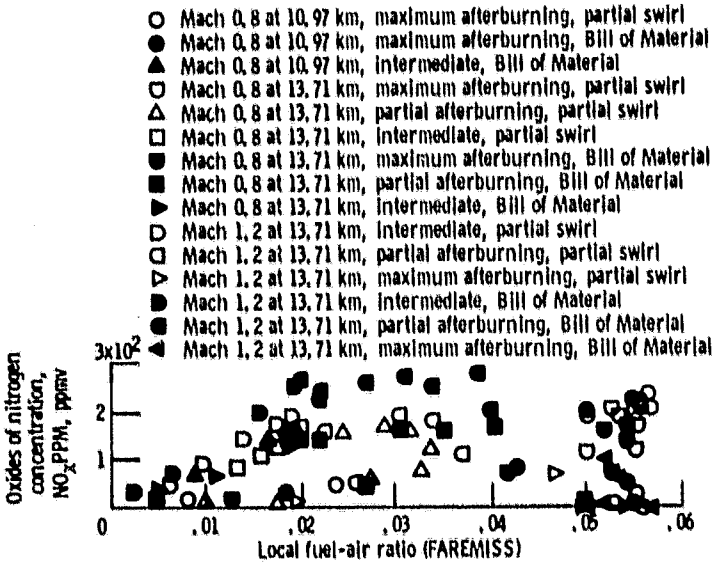

Figure 16. - Variation of oxides of nitrogen with gas sample fuel-air ratio.